

Generalized Low-Rank Matrix Contextual Bandits with Graph Information

Yao Wang

School of Management, Xi'an Jiaotong University, Xi'an, China, yao.s.wang@gmail.com

Jiannan Li

School of Management, Xi'an Jiaotong University, Xi'an, China, jiannanli@stu.xjtu.edu.cn

Yue Kang

Microsoft, Washington, United States, yuekang@microsoft.com

Shanxing Gao

School of Management, Xi'an Jiaotong University, Xi'an, China, gaozn@mail.xjtu.edu.cn

Zhenxin Xiao

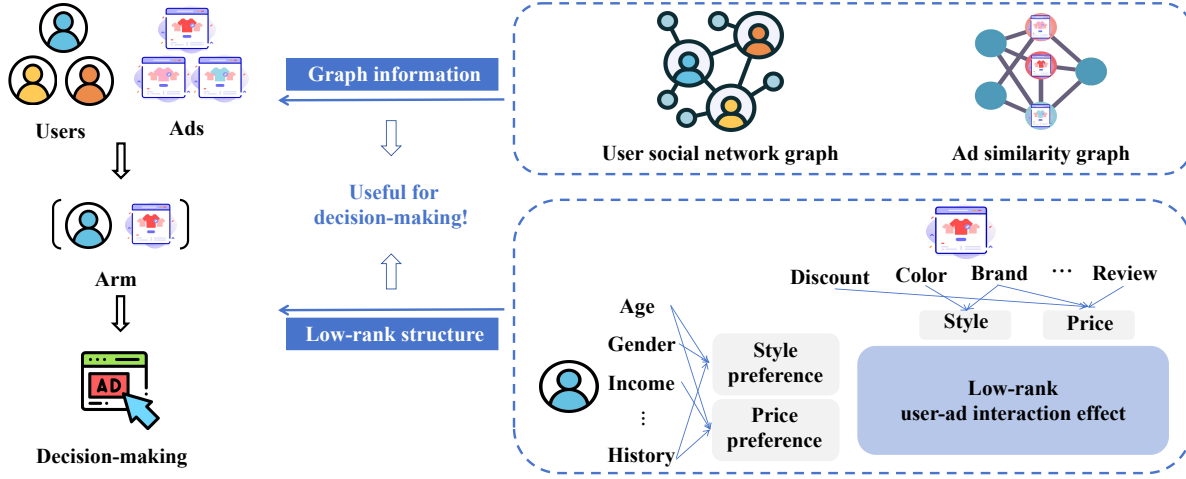
School of Management, Xi'an Jiaotong University, Xi'an, China, zxxiao@mail.xjtu.edu.cn

Abstract. The matrix contextual bandit (CB), as an extension of the well-known multi-armed bandit, is a powerful framework that has been widely applied in sequential decision-making scenarios involving low-rank structure. In many real-world scenarios, such as online advertising and recommender systems, additional graph information often exists beyond the low-rank structure, that is, the similar relationships among users/items can be naturally captured through the connectivity among nodes in the corresponding graphs. However, existing matrix CB methods fail to explore such graph information, and thereby making them difficult to generate effective decision-making policies. To fill in this void, we propose in this paper a novel matrix CB algorithmic framework that builds upon the classical upper confidence bound (UCB) framework. This new framework can effectively integrate both the low-rank structure and graph information in a unified manner. Specifically, it involves first solving a joint nuclear norm and matrix Laplacian regularization problem, followed by the implementation of a graph-based generalized linear version of the UCB algorithm. Rigorous theoretical analysis demonstrates that our procedure outperforms several popular alternatives in terms of cumulative regret bound, owing to the effective utilization of graph information. A series of synthetic and real-world data experiments are conducted to further illustrate the merits of our procedure.

Key words: sequential decision-making, matrix contextual bandits, graph information, generalized linear model

1. Introduction

The multi-armed bandit (MAB) has proven to be an effective framework for sequential decision-making, where the decision-maker progressively selects actions (i.e., arms) based on the historical data and the current state of the environment to maximize cumulative revenue (i.e., reward). However, traditional MAB approaches are limited in their ability to handle complex real-world tasks, such as user privacy protection (Han et al. 2020) or personalized decision-making (Zhou et al. 2023). This paper focuses on the latter by incorporating contextual information (e.g., user and item features), a setting known as the contextual bandit (CB) (Li et al. 2010, Chu et al. 2011). Due to more informed and adaptive decisions, CB methods have been widely applied across various

Figure 1 Illustration of Online Advertising in Social Networks.

domains, including recommender systems (Bastani et al. 2022, Aramayo et al. 2023), precision medicine (Bastani and Bayati 2020, Zhou et al. 2023), among others (Chen et al. 2020, Agrawal et al. 2023).

However, in some complex real-world applications, there are often significant interactions between user and item features that such vector representation based CBs are unable to effectively capture, leading to reduced decision accuracy. Taking the problem of online advertising in social networks as an example (as shown in Figure 1), the platform, as the decision-maker, needs to progressively adjust its advertisement (ad) delivery strategies based on historical data and environmental feedback to maximize long-term revenue, making this inherently a sequential decision-making problem. In this problem, users exhibit individual differences in features namely age, gender, income, and historical behavior, resulting in varied responses to the same ad features. For example, high-income users tend to prefer well-known brands, whereas low-income users may be more price-sensitive and less brand-dependent. This indicates that there are intricate interactions between ad features (e.g., discount, color, brand, and review) and the aforementioned user features. As such, traditional CBs simply stack the user and ad features into a joint feature vector cannot sufficiently model the underlying multi-dimensional relationships. Instead, adopting a matrix-based modeling approach provides a more effective alternative. Precisely, the rows and columns of the matrix correspond to users and ads, respectively, allowing for a more systematic representation of their interactions. Furthermore, the influence of these interactions on click behavior can be modeled through a small set of low-dimensional latent factors (e.g., style and price) significantly lower than the dimension of the feature matrix. This indicates that this problem exhibits a low-rank structure,

and should be handled by some designed matrix type of CB algorithms. This has also been explored in several other related problems, e.g., Cai et al. (2023), Lee et al. (2024).

In addition to the contextual information that describes the features of an action, some certain side information is often available, capturing the similarities among different actions. This kind of relationship is typically represented as an undirected graph (LeJeune et al. 2020, Thaker et al. 2022), where the nodes correspond to the actions, and the edges indicate their correlations. Consequently, this side information is commonly referred to as graph information. Continuing with the aforementioned online advertising example (as shown in the upper right of Figure 1), advertisers can take advantage of user interaction data on social media to build a social network (Zhou et al. 2020b) while also establishing a similarity graph between ads based on their click frequencies (Han et al. 2023). These graph structures reveal the impact of correlations on revenue: (1) Social connections between users often indicate similar interests, meaning that friends are more likely to be interested in the same type of ads; (2) Similarities between ads often indicate substitutability, meaning that ads for products of a similar style or price tend to attract the same user. Leveraging these insights, one can recommend similar ads to users who have a social connection with the user who clicked the ad, increasing the likelihood of purchase, and thus boosting revenue of decision-maker.

Basically, both low-rank structure and graph information are two important side information for providing effective decision-making procedures in online advertising problem and beyond, e.g., Lee et al. (2024), Abdallah et al. (2025). However, current popular bandit algorithms typically focus on exploiting just one aspect, that is, either the low-rank structure (Lu et al. 2021, Kang et al. 2022, Jang et al. 2024) or the graph information (Cesa-Bianchi et al. 2013, Kocák et al. 2020, Yang et al. 2020). Therefore, how to effectively leverage both types of information in a unified bandit framework and further improve the decision-making performance is the main focus of this study. To this end, we shall devise a new matrix CB algorithm. Specifically, we ingeniously integrate a matrix Laplacian regularization with the low-rank matrix structure into a unified way. Furthermore, it is worth noting that the rewards of CBs are not necessarily continuous variables in some practical applications, such as the binary rewards in recommender systems and the count based rewards in ad searches. This highlights the need for more flexible generalized linear models in this new CB algorithm. Our main contributions can be summarized as follows:

1. Methodologically, we introduce a novel CB algorithmic framework that effectively leverages both the low-rank structure and graph information inherent in complex decision-making scenarios. By solving an optimization problem that incorporates both the joint nuclear norm and a designed

matrix Laplacian regularizer, the proposed algorithm effectively integrates both types of information while maintaining high flexibility, unifying the reward relationships under different types of non-linearity, and thus being widely applicable to a range of real decision-making problems.

2. Theoretically, we use the typical cumulative regret to measure the gap between the decisions made by the proposed algorithm and the optimal decision. Through representing the sum of the aforementioned two regularization terms as an equivalent atomic norm, we can directly leverage the existing framework to derive a tighter cumulative regret bound, which includes a graph-related factor in the numerator to reflect the richness of graph information. That is, the factor decreases as the amount of graph information increases, leading to a tighter bound and highlighting the importance of leveraging such graph information. Additionally, this bound is independent of the number of actions, thus avoiding performance degradation in large action spaces.

3. Experimentally, we demonstrate the effectiveness of our proposed algorithm by comparing the numerical results with those of existing related algorithms. We evaluate these algorithms in various synthetic scenarios including the amount of graph information, different ranks, the number of actions and further in several real-world decision-making scenarios across cancer treatment, movie recommendation and ad searches. The extensive results show that the proposed algorithm achieves more accurate decision-making policies, as evidenced by a reduction in cumulative regret and an improvement in the optimal action hit rate.

1.1. Related Literature

1.1.1. Low-Rank Matrix Bandits A natural and intuitive method to develop matrix bandits is to directly generalize the multi-armed bandits from the vector representation to the matrix representation (Kveton et al. 2017, Katariya et al. 2017, Trinh et al. 2020). However, this type of method does not exploit feature information from the environment, making it difficult to achieve good decision-making performance in some complex scenarios. To address this issue, Jun et al. (2019) proposed bilinear bandits, which can be viewed as a contextual low-rank matrix bandit. Building upon this work, Jang et al. (2021) followed the bilinear setting and further leveraged the geometry of the action space to achieve an improved regret bound in terms of the matrix rank. As an extension of the aforementioned works, Lu et al. (2021) focused on a broader class of low-rank bandits, that is, generalized linear bandit models. However, its algorithm design relies on calculating covering numbers of low-rank matrices, which often suffer from computational intractability. To tackle this limitation, Kang et al. (2022) proposed a novel optimization objective for parameter estimation,

leading to a better regret bound in terms of feature dimension. To handle heavy-tailed noise in practice, Kang et al. (2024) developed a new estimator to improve model robustness and performance. However, all the aforementioned algorithms assume that an effective exploration distribution is given, which often cannot be satisfied in practice. To this end, Jang et al. (2024) introduced an experimental design approach to guide the selection of the exploration distribution and derived a regret bound related to the action set.

1.1.2. Bandits with Graph Information The first category of approaches for integrating graph information into the bandit framework comprises clustering based methods. Specifically, a series of works (Gentile et al. 2014, Korda et al. 2016, Yang and Toni 2018, Wang et al. 2023) segment users into distinct clusters and subsequently apply corresponding bandit algorithms to each user group. This process could effectively reduce the number of users that need to be individually managed, thereby enhancing overall performance. Besides, another line of works (Li et al. 2016, Gentile et al. 2017) considered the possibility that both users and items exhibit clustering structures, and proposed a double-clustering framework accordingly. However, such methods often overlook intra-cluster differences, which may lead to the loss of important features associated with key users or items. As such, the graph Laplacian regularization based methods (Cesa-Bianchi et al. 2013, Kocák et al. 2020, Yang et al. 2020) were proposed. By integrating some designed graph Laplacian regularizers into the optimization problem for parameter estimation, these methods enhance the accuracy of reward estimation within the bandit framework, thereby facilitating more precise decision-making. In this line of works, they primarily focus on user similarity, assuming that each user is associated with an individual parameter vector. Accordingly, their Laplacian regularization terms are designed to quantify the global impact of user similarity on the parameter matrix, where the i -th row represents the parameter vector of the i -th user. In contrast, Kocák et al. (2020) emphasizes item similarity under the assumption that all items share a common parameter vector, and the corresponding Laplacian regularization is used to quantify the effect of item similarity on rewards. With the advancements of deep learning techniques, some recent works (Qi et al. 2022, 2023) introduce Graph Neural Networks into the reward estimation process of the bandit framework by propagating and aggregating information over similarity graphs, thereby enhancing overall decision-making performance. These works still focus on single-aspect graph information, i.e., item similarity graph (Qi et al. 2022) or user similarity graph (Qi et al. 2023). However, in real-world applications, these two aspects (i.e., dual-graph information) can be captured simultaneously. Therefore, the

aforementioned single-perspective modeling approach leads to insufficient exploitation of graph information.

Although existing studies have provided important inspiration for this work, there remain significant differences. This work mainly focuses on more complex real-world scenarios where both low-rank structure and graph information are available simultaneously, whereas the aforementioned related works typically consider only one aspect—either emphasizing low-rankness or focusing on graph information. Moreover, this work further considers the coexistence of user and item similarity, which necessitates the design of new Laplacian regularization term to effectively model such dual-graph information.

1.2. Notations and Preliminaries

We first summarize the notations used throughout this paper. The symbols a , \mathbf{a} , A , and \mathcal{A} represent scalars, vectors, matrices, and sets, respectively. For a vector \mathbf{a} , $\|\mathbf{a}\|$ represents the l_2 -norm and $\|\mathbf{a}\|_M = \sqrt{\mathbf{a}^\top M \mathbf{a}}$ denotes the weighted norm. For a matrix A , $\|A\|_F$ represents the Frobenius norm, $\|A\|$ denotes the operator norm, and $\|A\|_*$ is the nuclear norm. For the operator symbols, \odot represents the outer product of the vectors, \otimes denotes the Kronecker product, and $\langle \cdot \rangle$ is the inner product of the vectors or matrices. $\mathcal{O}(\cdot)$ represents ignoring irrelevant constants and $\tilde{\mathcal{O}}(\cdot)$ denotes hiding logarithmic factors.

In the following, we shall introduce three key definitions.

DEFINITION 1 (TRUNCATED FUNCTION OF RECTANGULAR MATRIX (MINSKER 2018)). For the real-value function $\psi(\cdot): \mathbb{R} \rightarrow \mathbb{R}$ is defined as

$$\psi(x) = \begin{cases} \log(1 + x + \frac{x^2}{2}) & x \geq 0, \\ -\log(1 - x + \frac{x^2}{2}) & x < 0, \end{cases}$$

and rectangular matrix $A \in \mathbb{R}^{d_1 \times d_2}$, let $d = d_1 + d_2$, define

$$\psi_\nu(A) = \frac{[H \text{diag}(\psi(D_{11}), \dots, \psi(D_{dd})) H^\top]_{1:d_1, (d_1+1):d}}{\nu},$$

where $\nu > 0$, D_{ii} represents the i -th diagonal element of the matrix D . Matrices H, D are obtained from the full singular value decomposition (SVD) of $\tilde{A} = HDH^\top$, where $\tilde{A} \triangleq \begin{pmatrix} 0 & \nu A \\ \nu A^\top & 0 \end{pmatrix}$.

DEFINITION 2 (SCORE FUNCTION (KANG ET AL. 2022)). The score function is defined as $S(x) = -\nabla_x \log(p(x)) = -\nabla_x p(x)/p(x)$, where $p(x)$ is the probability density, $\nabla_x p(x)$ is the gradient of $p(x)$ with respect to the variable x . For the matrix X , the score function is defined as $S(X) = (S(X_{ij}))$.

DEFINITION 3 (WEIGHTED ATOMIC NORM (RAO ET AL. 2015)). For matrix $Z \in \mathbb{R}^{d_1 \times d_2}$, the weighted atomic norm with respect to the atomic set $\mathcal{A} \triangleq \{\omega_i \mathbf{h}_i^\top : \omega_i = A \mathbf{u}_i, \mathbf{h}_i = B \mathbf{v}_i, \|\mathbf{u}_i\| = \|\mathbf{v}_i\| = 1\}$ is defined as $\|Z\|_{\mathcal{A}} = \inf \sum_i |c_i|$ s.t. $Z = \sum_i c_i A_i$, $A_i \in \mathcal{A}$, where $A = PS_p^{-1/2}$, $B = QS_q^{-1/2}$, P, Q are the basis matrices spanning the matrix space, S_p, S_q are diagonal matrices whose diagonal elements correspond to the respective weights.

1.3. Organization of This Paper

The remainder of the paper is organized as follows. Section 2 provides a detailed formulation the studied problem. Section 3 presents the proposed algorithm, discussing its design principles and implementation details. Section 4 analyzes the theoretical results of the proposed algorithm, outlining key assumptions and regret bound. Section 5 evaluates the effectiveness and superiority of our algorithm through conducting a series of experiments. Finally, Section 6 summarizes the paper, highlights the research findings, and presents potential directions for future work.

2. Problem Formulation

In this section, we shall formally formulate the studied problem. Precisely, at each time step t , the decision-maker needs to select an item to display to the current user. Accordingly, the chosen action is represented as a specific (user, item) pair. Meanwhile, the decision-maker can observe the features of both the user and the item, denoted $\mathbf{p}_t \in \mathbb{R}^{d_1}$ and $\mathbf{q}_t \in \mathbb{R}^{d_2}$, respectively. The corresponding action can also be represented as a feature matrix $X_t = \mathbf{p}_t \odot \mathbf{q}_t \in \mathbb{R}^{d_1 \times d_2}$.

In addition to the features described above, real-world applications often involve another side information in the form of a graph that captures the similarity among different actions. This graph information can be either explicitly provided, such as user similarity constructed from a known social network, or implicitly inferred, for example, by applying methods such as k -nearest neighbor, ϵ -nearest neighbor to construct item similarity. We model this similarity information as an undirected graph $\mathcal{G} = (\mathcal{V}, \mathcal{E})$, where the node set $\mathcal{V} = \{1, 2, \dots, n\}$ represents all possible actions, and the edge set \mathcal{E} encodes pairwise similar relationships.

Moreover, the decision-maker interacts with the environment, subsequently obtaining the so-called reward, y_t . Considering the diverse nature of reward variables—such as binary variables (e.g., whether a movie is watched) in movie recommendation, continuous variables (e.g., treatment effectiveness) in precision medicine, and count variables (e.g., click-through rates) in ad searches—we can naturally assume that the relationship between the selected action and the reward belongs to the canonical exponential family defined as

$$p(y_t | X_t, \Theta^*) = \exp \left(\frac{y_t \langle X_t, \Theta^* \rangle - b(\langle X_t, \Theta^* \rangle)}{\phi} + c(y_t, \phi) \right),$$

$$\mathbb{E}(y_t | X_t, \Theta^*) = b'(\langle X_t, \Theta^* \rangle) \triangleq \mu(\langle X_t, \Theta^* \rangle),$$

where $\Theta^* \in \mathbb{R}^{d_1 \times d_2}$ is an unknown parameter, ϕ is the dispersion parameter, $b(\cdot)$ is a known and strictly convex log-partition function, the first derivative of $b(\cdot)$, i.e., $\mu(\cdot)$, is called the inverse link function. The above equation can be rewritten in the form of a generalized linear model as $y_t = \mu(\langle X_t, \Theta^* \rangle) + \epsilon_t$, where ϵ_t is the independent sub-Gaussian noise with parameter ω .

We begin by analyzing the impact of feature information on the reward, which is reflected in the low-rank structure of the parameter matrix Θ^* . As mentioned previously, the reward can be modeled using a small number of low-dimensional latent factors, which are determined by the interactions between users and items. These key latent factors represent the dominant directions of interaction and are captured by the eigenspace of Θ^* . In other words, the informative part of Θ^* is concentrated in a low-dimensional subspace that is much smaller than the original space (i.e., $\min\{d_1, d_2\}$), that is, Θ^* exhibits a typical low-rank structure with rank $r \ll \min\{d_1, d_2\}$.

This low-rank structure has led to a line of research on low-rank matrix contextual bandits (Kang et al. 2022, Jang et al. 2024), where decisions are made solely based on current feature information and historical observations. However, in real-world scenarios such as social networks, each user can be represented not only by a feature vector (e.g., demographic attributes) but also by a graph that encodes user connections (e.g., friendships or interactions). Similar relational structures can also be found among items. To this end, our setting additionally leverages such relational information by introducing an undirected graph \mathcal{G} over actions, which induces smoothness in the expected reward function. Specifically, for any two actions $i, j \in \mathcal{V}$, the difference in their expected rewards can be bounded by a graph-induced distance measure $d(\cdot, \cdot)$ about these actions, that is,

$$|\mu(\langle X_i, \Theta^* \rangle) - \mu(\langle X_j, \Theta^* \rangle)| \leq d(i, j),$$

where $d(\cdot, \cdot)$ measures the similarity between actions. In essence, actions that are close in the graph tend to yield similar expected rewards. This enables more accurate decisions by leveraging information propagation across action connections and uncovering relationships beyond what feature matrices alone can capture. Importantly, our use of the graph differs fundamentally from prior works based on graph feedback (Gou et al. 2023, Gong and Zhang 2025), which assume that selecting an action reveals the rewards of its neighbors on the graph. In contrast, our approach does not require such side observations, which are often costly or impractical to obtain in real-world applications.

Based on the above analysis, then the main objective is to maximize the cumulative reward $\sum_{t=1}^T \mu(\langle X_t, \Theta^* \rangle)$. If Θ^* is known, one can easily choose the optimal action as $X^* \triangleq$

$\arg \max_{X \in \mathcal{X}} \mu(\langle X, \Theta^* \rangle)$, where \mathcal{X} is the action set. However, Θ^* is usually unknown in practice. Therefore, we reformulate the optimization goal to minimize the following cumulative regret

$$R_T = \sum_{t=1}^T [\mu(\langle X^*, \Theta^* \rangle) - \mu(\langle X_t, \Theta^* \rangle)], \quad (1)$$

which measures the gap between the actions $\{X_t\}_{t=1}^T$ selected by the proposed algorithm and the optimal action X^* .

3. Method

In this section, we shall develop an innovative algorithm named as ‘‘Graph-Generalized Explore Subspace Then Transform’’ (GG-ESTT) to minimize the cumulative regret defined in (1). Then the core challenge lies in the fact that the true parameter matrix Θ^* is unknown, necessitating the estimation involved in the decision-making process. Given that the unknown Θ^* exhibits a low-rank structure, we focus on estimating the column and row subspaces to fully exploit this structural characteristic. In addition, we shall further leverage the available graph information to improve the accuracy of such subspaces estimation. We then utilize the revealed space redundancy from this stage to transform the original space into an almost low-dimensional parameter space. Subsequently, in this transformed space, we continue to utilize graph information to design an efficient action selection strategy. The detailed procedure is summarized in Algorithm 1.

3.1. Estimation of Subspace with Graph Information

The first stage (lines 1-4) of the proposed Algorithm 1 is to leverage graph information for improving the estimation of the low-rank subspace. To this end, we use the observations up to time T_1 to obtain an initial estimate of the unknown parameter Θ^* by solving an optimization problem with two regularization terms capturing the low-rank structure and graph information, respectively. Specifically, due to the non-linearity of the reward function, we adopt a commonly-used quadratic loss function (Plan and Vershynin 2016, Yang et al. 2017), defined as

$$L_{T_1}(\Theta) \triangleq \langle \Theta, \Theta \rangle - \frac{2}{T_1} \sum_{i=1}^{T_1} \langle \psi_\nu(y_i \cdot S(X_i)), \Theta \rangle,$$

where $\psi_\nu(\cdot)$ and $S(\cdot)$ are given in Definitions 1 and 2, respectively. We then use the commonly used nuclear norm to characterize the low-rank structure, defined as

$$R_n(\Theta) \triangleq \|\Theta\|_* = \inf_{U, V} \{\|U\|_F + \|V\|_F : \Theta = UV^\top\}.$$

Algorithm 1 Graph-Generalized Explore Subspace Then Transform (GG-ESTT)**Input:** $\mathcal{X}, \lambda, \alpha, T_1, T, r, \tau, \lambda_2, \lambda_\perp, L$.

- 1: **for** $t = 1$ to T_1 **do**
- 2: Choose action $X_t \in \mathcal{X}$ according to distribution \mathbb{D} , and receive reward y_t .
- 3: **end for**
- 4: Compute the estimator $\hat{\Theta}_{T_1}$ by Equation (3).
- 5: Rotate the action set and parameter space as followed:

$$\mathcal{X}' = \left\{ (\hat{U}, \hat{U}_\perp)^\top X (\hat{V}, \hat{V}_\perp) : X \in \mathcal{X} \right\}, \Theta' = (\hat{U}, \hat{U}_\perp)^\top \Theta^* (\hat{V}, \hat{V}_\perp),$$

where $\hat{U} \in \mathbb{R}^{d_1 \times r}$, $\hat{U}_\perp \in \mathbb{R}^{d_1 \times d_1 - r}$, $\hat{V} \in \mathbb{R}^{d_2 \times r}$, $\hat{V}_\perp \in \mathbb{R}^{d_2 \times d_2 - r}$ are obtained from the full SVD of $\hat{\Theta}_{T_1} = (\hat{U}, \hat{U}_\perp) S (\hat{V}, \hat{V}_\perp)^\top$.

- 6: Obtain the vectorized parameter θ^* and its corresponding action set $\mathcal{X}'_{\text{vec}}$ according to (5) and (6), respectively, such that the last $(d_1 - r) \cdot (d_2 - r)$ components lie in the redundant space.
- 7: **for** $t = 1$ to $T_2 = T - T_1$ **do**
- 8: Run Graph-LowGLM-UCB (Algorithm 2) with action set $\mathcal{X}'_{\text{vec}}$ and the low dimension $k = (d_1 + d_2 - r)r$.
- 9: **end for**

In contrast, existing graph Laplacian regularizations only reflect the single-aspect graph information based on either user similarity or item similarity, which cannot be used to characterize the dual-graph information considered in this work.

We shall further show how to characterize such dual-graph information in our algorithm. For the action set \mathcal{G} , the similarity between actions can be captured by a symmetric matrix W (i.e., the adjacency matrix), where $W_{ij} = 1$ indicates that action i and action j are similar (i.e., connected) and $W_{ij} = 0$ otherwise. Then, the graph Laplacian matrix of \mathcal{G} is defined as $L \triangleq D - W$, where D is the diagonal matrix with entries $d_{ii} \triangleq \sum_j W_{ij}$ (node degrees). With these notions, we propose a graph Laplacian regularization, which measures the smooth variation of the expected rewards over the entire action set, that is,

$$R_L(\Theta^*) \triangleq \frac{1}{2} \sum_{ij} W_{ij} [\mu(\langle X_i, \Theta^* \rangle) - \mu(\langle X_j, \Theta^* \rangle)]^2 = a_\mu \text{tr} \left\{ \Theta^{*\top} \tilde{X}^\top L \tilde{X} \Theta^* \right\}, \quad (2)$$

where $\tilde{X} \triangleq (\text{vec}(X_1), \text{vec}(X_2), \dots, \text{vec}(X_n))^\top$. The constant a_μ is constrained by the bound of the first derivative of μ . Noting that each action feature X_i is a user-item interaction matrix, where rows

and columns correspond to user and item features, respectively. Thus, X_i simultaneously encodes information from both the user and the item. By stacking all these action features, the resulting matrix \tilde{X} serves as a joint representation of the entire action set, comprising all (user, item) pairs. Combining with the graph Laplacian matrix L to encode the similarity structure among actions, this regularization term can effectively model the inherent smoothness over the dual-graph structure.

Based on the above formulation, we can obtain the estimated parameter $\hat{\Theta}_{T_1}$ by

$$\hat{\Theta}_{T_1} = \arg \min_{\Theta \in \mathbb{R}^{d_1 \times d_2}} L_{T_1}(\Theta) + \lambda R_n(\Theta) + \alpha R_L(\Theta), \quad (3)$$

where λ and α are the tuning parameters to control the influence of their corresponding regularization terms. We then perform a full SVD on the estimated $\hat{\Theta}_{T_1}$, that is, $\hat{\Theta}_{T_1} = (\hat{U}, \hat{U}_\perp) \hat{S} (\hat{V}, \hat{V}_\perp)^\top$, where $\hat{U} \in \mathbb{R}^{d_1 \times r}$, $\hat{U}_\perp \in \mathbb{R}^{d_1 \times (d_1 - r)}$, $\hat{V} \in \mathbb{R}^{d_2 \times r}$, and $\hat{V}_\perp \in \mathbb{R}^{d_2 \times (d_2 - r)}$. It is easy to see that \hat{U} and \hat{V} are the column and row subspaces of $\hat{\Theta}_{T_1}$, which consist its top r left and right singular vectors, respectively. These subspaces provide a natural estimate of the corresponding subspaces of the true parameter matrix Θ^* .

Considering the space redundancy revealed by the above subspace estimation, we further transform the original parameter space into an almost low-dimensional space (i.e., the lines 5-6 of Algorithm 1) to reduce the cumulative regret. More precisely, this can be done in two steps, i.e., orthogonal rotation and vectorized rearrangement. Specifically, orthogonal rotation refers to projecting the true parameter Θ^* onto the orthogonal space spanned by all singular vectors of the estimated $\hat{\Theta}_{T_1}$. This gives a rotated version of Θ^* , defined as $\Theta' = (\hat{U}, \hat{U}_\perp)^\top \Theta^* (\hat{V}, \hat{V}_\perp)$. To ensure the equivalence of the problem, it is necessary to reformulate the expected reward as

$$\mu(\langle X, \Theta^* \rangle) = \mu \left(\text{tr} \left\{ \left[(\hat{U}, \hat{U}_\perp)^\top X (\hat{V}, \hat{V}_\perp) \right]^\top \Theta' \right\} \right) = \mu(\langle X', \Theta' \rangle), \quad (4)$$

from which we get the rotated action set $\mathcal{X}' = \left\{ (\hat{U}, \hat{U}_\perp)^\top X (\hat{V}, \hat{V}_\perp) : X \in \mathcal{X} \right\}$. We then rearrange $\text{vec}(\Theta')$ such that the first $k \triangleq (d_1 + d_2 - r)r$ elements are in the subspace, while the remaining elements are in the orthogonal complement, which is explicitly given by

$$\theta^* = \left(\text{vec} \left(\Theta'_{1:r, 1:r} \right); \text{vec} \left(\Theta'_{r+1:d_1, 1:r} \right); \text{vec} \left(\Theta'_{1:r, r+1:d_2} \right); \text{vec} \left(\Theta'_{r+1:d_1, r+1:d_2} \right) \right), \quad (5)$$

and denote the corresponding action set as

$$\mathcal{X}'_{\text{vec}} = \left\{ \left(\text{vec} \left(X'_{1:r, 1:r} \right); \text{vec} \left(X'_{r+1:d_1, 1:r} \right); \text{vec} \left(X'_{1:r, r+1:d_2} \right); \text{vec} \left(X'_{r+1:d_1, r+1:d_2} \right) \right) : X' \in \mathcal{X}' \right\}. \quad (6)$$

Algorithm 2 Graph-LowGLM-UCB**Input:** $\mathcal{X}'_{\text{vec}}, T_2, k, L, \alpha, \delta, \tau, \lambda_2, \lambda_{\perp}, c_{\mu}, a_{\mu}, k_{\mu}, \omega$.

- 1: Let $\Lambda = \text{diag}(\lambda_2, \dots, \lambda_2, \lambda_{\perp}, \dots, \lambda_{\perp})$, where λ_2 occupies the first k diagonal entries; $V(c_{\mu}) = \frac{\Lambda + a_{\mu} \alpha \tilde{X}^{\top} L \tilde{X}}{c_{\mu}}$; $V_1(c_{\mu}) = V(c_{\mu}) + \sum_{i=1}^{T_1} \mathbf{x}_{h,i} \mathbf{x}_{h,i}^{\top}$, where the data $\{\mathbf{x}_{h,i}\}_{i=1}^{T_1}$ collected in the subspace estimation.
- 2: **for** $t = 1$ to T_2 **do**
- 3: Compute $\hat{\theta}_t$ according to Equation (7).
- 4: Choose action $\mathbf{x}_t = \arg\max_{\mathbf{x} \in \mathcal{X}'_{\text{vec}}} \left\{ \mu(\langle \hat{\theta}, \mathbf{x} \rangle) + \frac{k_{\mu}}{c_{\mu}} e_t \|\mathbf{x}\|_{V_t^{-1}(c_{\mu})} \right\}$ and receive reward y_t ,
 where $e_t = \omega \sqrt{\log \frac{|V_t(c_{\mu})|}{|V(c_{\mu})| \delta^2}} + \sqrt{c_{\mu}} (\sqrt{\lambda_2} + \sqrt{\lambda_{\perp}} \tau + 1)$.
- 5: Update $V_{t+1}(c_{\mu}) = V_t(c_{\mu}) + \mathbf{x}_t \mathbf{x}_t^{\top}$.
- 6: **end for**

Then it is not hard to see that the orthogonal complements $\hat{U}_{\perp}, \hat{V}_{\perp}$ of the estimated subspaces can be used to assess the redundancy in the transformed parameter θ^* . Specifically, we have

$$\begin{aligned} \|\theta_{k+1:d_1 d_2}^*\|^2 &= \sum_{i>r, j>r} \Theta_{ij}^{\prime 2} = \|\hat{U}_{\perp}^{\top} (U^* S^* V^{*\top}) \hat{V}_{\perp}\|_F^2 \leq \|\hat{U}_{\perp}^{\top} U^*\|_F^2 \|S^*\|^2 \|\hat{V}_{\perp}^{\top} V^*\|_F^2 \\ &\leq \|\hat{U}_{\perp}^{\top} U^*\|_F^2 \|\hat{V}_{\perp}^{\top} V^*\|_F^2, \end{aligned}$$

where $U^* \in \mathbb{R}^{d_1 \times r}$, $S^* \in \mathbb{R}^{r \times r}$, and $V^* \in \mathbb{R}^{d_2 \times r}$ are obtained from the truncated SVD of the true parameter matrix $\Theta^* = U^* S^* V^{*\top}$. The above inequality shows that the more accurate the estimated subspaces are, the tail of the transformed parameter vector θ^* tends to 0, indicating that the transformed parameter θ^* lies in an almost low-dimensional space. This dimensionality reduction effectively reduces the complexity of the parameter space and lays the foundation for designing an efficient action selection strategy within this almost low-dimensional space.

3.2. Graph-Based Action Selection Strategy

In the second stage (lines 7-9) of proposed Algorithm 1, we shall design an efficient action selection strategy named as Graph-LowGLM-UCB for the transformed parameter space, which integrates graph information under the framework of classical upper confidence bound (UCB) algorithm. The main objective of such UCB algorithm is to construct a confidence interval for the expected reward of each candidate action and select the action with the highest upper confidence bound. One can refer to Algorithm 2 for specific details.

In the transformed low-dimensional space, the observation model can be equivalently reformulated as $y_t = \mu(\langle \mathbf{x}_t, \theta^* \rangle) + \epsilon_t$, where the action $\mathbf{x}_t \in \mathcal{X}'_{\text{vec}}$ and the noise ϵ_t is an independent

sub-Gaussian variable with parameter ω . The forms of the true transformed parameter θ^* and the corresponding action set $\mathcal{X}'_{\text{vec}}$ have been given in (5) and (6), respectively. Considering that θ^* is unknown in practice, it is necessary to provide a good estimate of it.

Importantly, the first stage of the proposed Algorithm 1 provides prior information that $\|\theta^*_{k+1:d_1d_2}\| \leq \tau$, where τ is the error bound of the subspace estimation. Using this prior, we can explicitly separate the informative low-rank part $\theta^*_{1:k}$ from the redundant residual part $\theta^*_{k+1:d_1d_2}$ to obtain a better estimation of unknown θ^* . Specifically, we introduce a diagonal matrix $\Lambda = \text{diag}(\lambda_2, \dots, \lambda_2, \lambda_\perp, \dots, \lambda_\perp)$, which imposes different levels of penalization on the two aforementioned parts of the parameter θ^* . The first k diagonal entries are set to λ_2 , while the remaining entries are set to λ_\perp . Building on this, we further incorporate the previously introduced Laplacian regularization term defined in Equation (2), leading to the final form of the minimization problem (maximum likelihood with regularizations), which is formulated as

$$\begin{aligned} \hat{\theta}_t = \arg \min_{\theta \in \mathbb{R}^{d_1d_2}} & \sum_{i=1}^{T_1} [b(\langle \mathbf{x}_{h,i}, \theta \rangle) - y_{h,i} \langle \mathbf{x}_{h,i}, \theta \rangle] + \sum_{i=1}^{t-1} [b(\langle \mathbf{x}_i, \theta \rangle) - y_i \langle \mathbf{x}_i, \theta \rangle] \\ & + \frac{1}{2} \|\theta\|_\Lambda^2 + \frac{a_\mu \alpha}{2} \theta^\top \tilde{X}^\top L \tilde{X} \theta. \end{aligned} \quad (7)$$

Here, we reuse the historical data from stage 1, $\{\mathbf{x}_{h,i}, y_{h,i}\}_{i=1}^{T_1}$, to increase the sample size in stage 2, thereby improving the accuracy of parameter estimation $\hat{\theta}_t$.

Based on the above parameter estimation $\hat{\theta}_t$, we select actions according to the UCB principle, as described in line 4 of Algorithm 2. Specifically, for each candidate action \mathbf{x} , we construct an optimistic estimate of its reward defined as $\mu(\langle \hat{\theta}_t, \mathbf{x} \rangle) + w_t$, where the first term $\mu(\langle \hat{\theta}_t, \mathbf{x} \rangle)$ denotes the estimated expected reward, capturing the exploitation behavior based on historical observations, while the second term w_t represents the confidence width, quantifying the uncertainty of the estimate. We then select the action with the highest optimistic estimate from the available candidates, that is,

$$\mathbf{x}_t = \arg \max_{\mathbf{x} \in \mathcal{X}'_{\text{vec}}} \left\{ \mu(\langle \hat{\theta}_t, \mathbf{x} \rangle) + w_t \right\}, \quad (8)$$

where the explicit form of w_t will be derived in the subsequent theoretical analysis.

4. Theory

In this section, we shall present a theoretical analysis in terms of the cumulative regret bound for the proposed algorithm, highlighting the significant role of graph information for improving such a bound. To this end, we begin by presenting the key and mild assumptions required for the analysis.

We then establish the subspace estimation error bound with graph information. Next, we derive an explicit expression of the confidence width w_t in (8), which leads to the regret bound for the graph-based action selection strategy, i.e., Algorithm 2. Finally, we combine these results to derive the overall cumulative regret bound of the proposed Algorithm 1.

4.1. Assumptions

In this subsection, we would like to introduce several necessary assumptions to facilitate subsequent theoretical analysis.

ASSUMPTION 1 (Feature Distribution). *There exists a sampling distribution \mathbb{D} over \mathcal{X} with its associated density $\mathbf{P} = (p_{ij}) : \mathbb{R}^{d_1 \times d_2}$, such that $\forall i, j$, the score function $S(\cdot)$ satisfies $\mathbb{E}[S^2(X_{ij})] \leq \gamma$, where the random matrix X is drawn from \mathbb{D} , that is, the probability density of X_{ij} is p_{ij} . The explicit form of $S(\cdot)$ is given in Definition 2.*

ASSUMPTION 2 (Bounded Norm). *The true parameter and feature matrices have a bounded norm, that is, $\|\Theta^*\|_F \leq 1, \|X\|_F \leq 1$, where $\forall X \in \mathcal{X}$.*

ASSUMPTION 3 (The Inverse Link Function). *The inverse link function $\mu(\cdot)$ is continuously differentiable and there exist two constants c_μ, k_μ such that $0 < c_\mu \leq \mu'(x) \leq k_\mu$ for all $|x| \leq 1$.*

Now we shall state that the above assumptions can be easily satisfied in practice. Specifically, Assumption 1 only requires the score function to have a finite second moment, which can be met by many common distributions such as Gaussian, exponential, and uniform distributions. Assumption 2, a boundedness condition commonly used in the bandits literature (e.g., Bastani and Bayati (2020), Lu et al. (2021)), can be easily satisfied by normalization. Assumption 3 is a standard assumption in generalized linear bandits (Kang et al. 2022, Yi et al. 2024), which only requires the first derivative of the inverse link function to be bounded. It is easy to check that the common generalized linear models, such as logistic and Poisson regression models, satisfy this condition.

4.2. Deriving Error Bound for Subspace Estimation with Graph Information

When applying existing CB analytical framework to derive error bound for parameter estimation, we observe that this framework is typically designed for a single regularization term. However, this work involves two regularization terms capturing the low-rank structure and graph information, respectively. Inspired by Rao et al. (2015), we equivalently represent the sum of these two regularization terms as a single atomic norm. To this end, we introduce the following lemma as a theoretical foundation for our analysis.

LEMMA 1. Let L_h and L_w denote the Laplacian matrices corresponding to the user and item similarity graphs, respectively, and let L be the Laplacian matrix corresponding to the (user, item) pair similarity graph. Suppose that $L_w = U_w S_w U_w^\top$ and $L_h = U_h S_h U_h^\top$ are the full SVD of L_w and L_h , respectively. Define the atomic set as

$$\mathcal{A} \triangleq \left\{ \omega_i \mathbf{h}_i^\top : \omega_i = A \mathbf{u}_i, \mathbf{h}_i = B \mathbf{v}_i, \|\mathbf{u}_i\| = \|\mathbf{v}_i\| = 1, A = U_w S_w^{-1/2}, B = U_h S_h^{-1/2} \right\}.$$

Assume that conditions $L_h = \lambda I, 2a_\mu \alpha (H^\top \otimes I) \tilde{X}^\top L \tilde{X} (H \otimes I) + \lambda I = I \otimes L_w$, are satisfied, where $W = U_\Theta S_\Theta^{\frac{1}{2}}, H = V_\Theta S_\Theta^{\frac{1}{2}}, \Theta = U_\Theta S_\Theta U_\Theta^\top$ is the full SVD of Θ , then the weighted atomic norm given in Definition 3 can be rewritten as $\|\Theta\|_{\mathcal{A}} = \inf_{\Theta} \left\{ \lambda \|\Theta\|_* + a_\mu \alpha \text{tr} \left\{ \Theta^\top \tilde{X}^\top L \tilde{X} \Theta \right\} \right\}$.

With the above lemma, the estimator $\hat{\Theta}_{T_1}$ in Equation (3) can be equivalently obtained by

$$\hat{\Theta}_{T_1} = \arg \min_{\Theta \in \mathbb{R}^{d_1 \times d_2}} \langle \Theta, \Theta \rangle - \frac{2}{T_1} \sum_{i=1}^{T_1} \langle \psi_{\nu}(y_i \cdot S(X_i)), \Theta \rangle + \beta \|\Theta\|_{\mathcal{A}}, \quad (9)$$

where β is the tuning parameter to control the influence of its corresponding regularization term. Then, we can further apply the existing CB analytical framework by separately handling the loss function and the single regularization term. This leads to the following theoretical bound.

THEOREM 1 (Error Bound for Parameter Estimation with Graph Information). Under Assumptions 1-3, and the conditions of Lemma 1. Consider the estimator $\hat{\Theta}_{T_1}$ in Equation (3) with $\lambda \leq 1$ and $\alpha \leq \frac{1-\lambda}{4a_\mu n(n-1)}$, or equivalently, the estimator $\hat{\Theta}_{T_1}$ in Equation (9) with

$$\nu = \sqrt{\frac{2 \log(2(d_1 + d_2)/\delta)}{(4\omega^2 + r_{\max}^2) \gamma T_1 \max\{d_1, d_2\}}}, \beta = 4\zeta \sqrt{\frac{2(4\omega^2 + r_{\max}^2) \gamma d_1 d_2 \log(2(d_1 + d_2)/\delta)}{T_1}}.$$

Then, with probability at least $1 - \delta$, the estimation error satisfies

$$\left\| \hat{\Theta}_{T_1} - \mu^* \Theta^* \right\|_F^2 \leq \frac{c_1 \zeta^2 d_1 d_2 \gamma r \log\left(\frac{2(d_1 + d_2)}{\delta}\right)}{T_1},$$

where $c_1 = 36(4\omega^2 + r_{\max}^2)$, $r_{\max} = |\mu(0)| + k_\mu$, $\mu^* = \mathbb{E}[\mu'(\langle X, \Theta^* \rangle)]$, and the constant $\zeta \in (0, 1]$ is related to the graph information.

Building on the above parameter estimation result, we further perform the full SVD on the estimated parameter as $\hat{\Theta}_{T_1} = (\hat{U}, \hat{U}_\perp) \hat{S} (\hat{V}, \hat{V}_\perp)^\top$ to quantify the estimation error of the low-rank parameter subspace.

COROLLARY 1 (Error Bound for Subspaces Estimation with Graph Information). Suppose $\hat{\Theta}_{T_1}$ is obtained from Equation (3) or Equation (9) as an estimate of the true parameter Θ^* . The matrices U^* and V^* are obtained from the truncated SVD of $\Theta^* = \hat{U}^* S^* V^{*\top}$. Under the conditions of Theorem 1, with probability at least $1 - \delta$, we have

$$\|\hat{U}_\perp^\top U^*\|_F \|\hat{V}_\perp^\top V^*\|_F \leq \frac{\|\mu^* \Theta^* - \hat{\Theta}\|_F^2}{c_r^2} \leq \frac{c_1 \zeta^2 d_1 d_2 \gamma r \log\left(\frac{2(d_1+d_2)}{\delta}\right)}{T_1 c_r^2},$$

where $c_r > 0$ denotes the lower bound of the r -th singular value of Θ^* and c_1 represents some constant.

Based on the above result, we achieve a more accurate estimation of the low-rank subspace. Compared to the error bound in Kang et al. (2022) that ignores the graph information, our bound incorporates a factor ζ smaller than 1 in the numerator, which leads to a significant reduction in estimation error. This improvement highlights the importance of integrating graph information into the low-rank subspace estimation process.

4.3. Analyzing Regret Bound for Graph-Based Action Selection Strategy

In analyzing the cumulative regret of an action selection strategy, it is essential to first explicitly characterize the confidence width of the estimated reward.

THEOREM 2 (The Confidence Width). Let $V(s) = \frac{\Lambda + a_\mu \alpha \tilde{X}^\top L \tilde{X}}{s}$, $V_t(s) = V(s) + \sum_{i=1}^{T_1} \mathbf{x}_{h,i} \mathbf{x}_{h,i}^\top + \sum_{k=1}^{t-1} \mathbf{x}_k \mathbf{x}_k^\top$. Assume that $\|\theta^*\| \leq 1$ and $\|\theta_{k+1:d_1 d_2}^*\| \leq \tau$. Then, under Assumptions 1-3, with probability at least $1 - \delta$, for all $t \geq 0$ and any action $\mathbf{x} \in X'_{vec}$, we have $\left| \mu(\langle \mathbf{x}, \theta^* \rangle) - \mu(\langle \mathbf{x}, \hat{\theta}_t \rangle) \right| \leq w_t$, where $w_t = \frac{k_\mu}{c_\mu} \|\mathbf{x}\|_{V_t^{-1}(c_\mu)} \left[\omega \sqrt{\log\left(\frac{|V_t(c_\mu)|}{|V(c_\mu)| \delta^2}\right)} + \sqrt{c_\mu} (\sqrt{\lambda_2} + \sqrt{\lambda_\perp} \tau + 1) \right]$.

Building on the above theorem, we further address the term $\log\left(\frac{|V_t(c_\mu)|}{|V(c_\mu)|}\right)$. Due to the incorporation of graph information, the matrix $V(c_\mu)$ is no longer diagonal as in Lemma 2 of Jun et al. (2019), making their result inapplicable. To address this issue, we extend the result to the general positive definite matrix and derive the regret by carefully choosing λ_\perp .

THEOREM 3 (The Regret of Graph-Based Action Selection). Under Assumptions 1-3, the regret of Graph-LowGLM-UCB with $\lambda_\perp = \frac{c_\mu T}{k \log(1 + \frac{c_\mu T}{\lambda_2})}$ is $\tilde{O}\left(\omega k \sqrt{T} + \tau T\right)$, with probability at least $1 - \delta$.

The regret in the above theorem depends on the effective dimension $k = (d_1 + d_2 - r)r$ instead of the original dimension $d_1 d_2$, resulting in a better bound. This improvement comes from explicitly separating the informative low-rank part from the redundant residual part, highlighting the benefit of transforming the problem into an almost low-dimensional space.

4.4. Deriving Overall Regret Bound

By combining the theoretical results of both preceding subsections, we derive the overall regret of the proposed Algorithm 1.

THEOREM 4 (Overall Regret). *Under Assumptions 1-3, suppose we run Algorithm 1 with $T_1 \geq \frac{\zeta \sqrt{d_1 d_2 \gamma r T}}{c_r}$, $\lambda_{\perp} = \frac{c_{\mu} T}{k \log(1 + \frac{c_{\mu} T}{\lambda_2^2})}$, $\tau = \frac{c_1 \zeta^2 d_1 d_2 \gamma r \log(\frac{2(d_1 + d_2)}{\delta})}{T_1 c_r^2}$, the overall regret is $\tilde{O}\left(\frac{\zeta \sqrt{d_1 d_2 \gamma r T}}{c_r}\right)$, with probability at least $1 - \delta$.*

Compared with existing methods, our regret offers two main advantages: (1) Compared to method that ignores graph information (Kang et al. 2022), our bound introduces a factor ζ in the numerator, which decreases with richer graph information, thereby reducing cumulative regret; (2) Compared to method that does not utilize low-rank structure (Yang et al. 2020), our bound is tighter for dimension d_2 and is independent of the number of users.

5. Experiments

In this section, we demonstrate the superior performance of our proposed Algorithm 1, GG-ESTT, through numerical experiments on both synthetic data and real-world data. All experimental evaluations were conducted on a computer equipped with an Intel(R) Xeon(R) Gold 5120 CPU @ 2.20GHz, using Python 3.9.

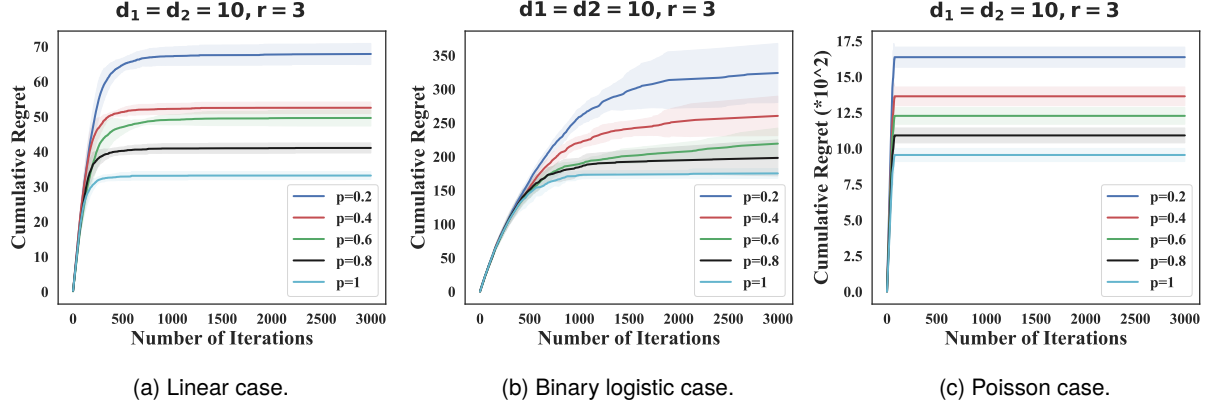
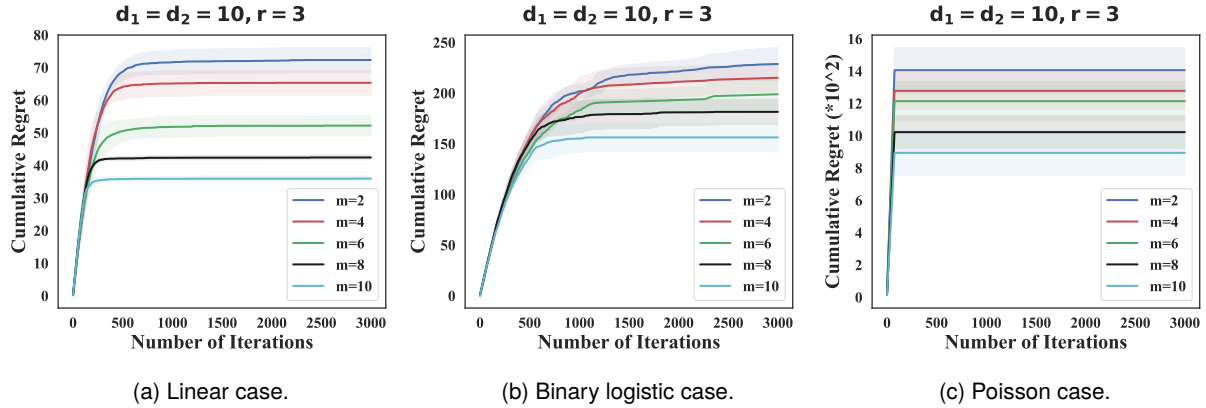
5.1. Synthetic Data Experiments

We generate a real parameter matrix Θ^* with dimensions $d_1 \times d_2$ as $\Theta^* = A M B^{\top}$, where $M = U V^{\top}$, $U \in \mathbb{R}^{d_1 \times r}$, $V \in \mathbb{R}^{d_2 \times r}$, and the elements are independently sampled from $N(0, 1)$. Specifically, the definitions of A and B can be found in Lemma 1. Regarding the action set \mathcal{X} , there are two generation methods:

- The impact of graph information richness: directly drawing n matrices with dimensions $d_1 \times d_2$, where the elements are independently sampled from $N(0, 1)$.
- Comparison with related algorithms: drawing n_1 and n_2 vectors independently from $N(\mathbf{0}, I_{d_1})$ and $N(\mathbf{0}, I_{d_2})$, respectively, to serve as feature vectors for item 1 and item 2. Subsequently, by computing the outer product of these vectors, we generate $n = n_1 n_2$ feature matrices, each corresponding to a (item 1, item 2) pair.

For each action $X_t \in \mathcal{X}$, the rewards are generated using three common generalized linear models:

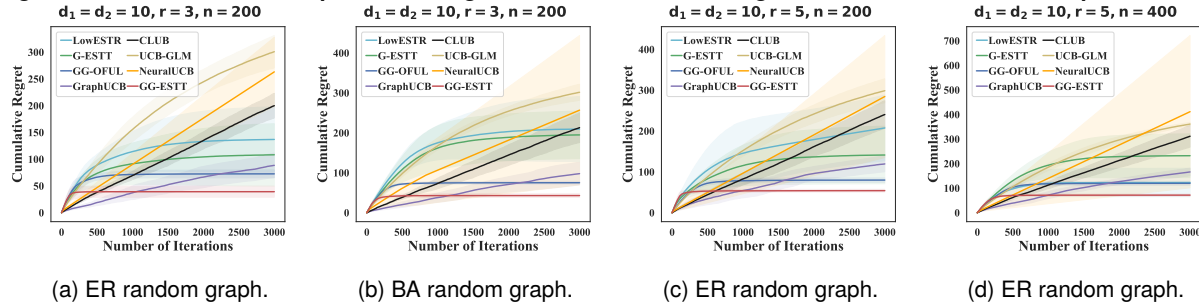
- Linear case: $y_t \sim N(\langle X_t, \Theta^* \rangle, \omega^2)$, where $\omega = 0.01$.
- Binary logistic case: $y_t \sim \text{Logistic}(p_t)$, where $p_t = \frac{1}{1 + e^{-\langle X_t, \Theta^* \rangle}}$.

Figure 2 ER Random Graph: the Impact of Graph Information Richness.**Figure 3 BA Random Graph: the Impact of Graph Information Richness.**

- Poisson case: $y_t \sim \text{Poisson}(\eta_t)$, where $\eta_t = e^{\langle X_t, \Theta^* \rangle}$.

For each simulation setting, we repeated the process 5 times to calculate the average regret at each time step and its standard deviation confidence interval.

5.1.1. The Impact of Graph Information Richness To better demonstrate the algorithm's ability to utilize graph information, we examine how the increase of similarity information in the graph affects the cumulative regret, under fixed the number of actions and parameter matrix settings. To this end, we construct the graph \mathcal{G} using two representative random graph models: (1) Erdős–Rényi (ER) random graph: Each pair of nodes is independently connected with probability p . (2) Barabási–Albert (BA) random graph: Starting from an initial connected graph with m nodes, new nodes are added to the graph one at a time, each forming m edges to existing nodes. The connections follow the principle of preferential attachment, whereby nodes with more edges have a greater probability of being selected for connection by the new node. As shown in Figure 2 (ER random graph) and Figure 3 (BA random graph), when other settings are fixed, the cumulative regret decreases as the parameter of the random graph model (i.e., p or m) increases. This trend

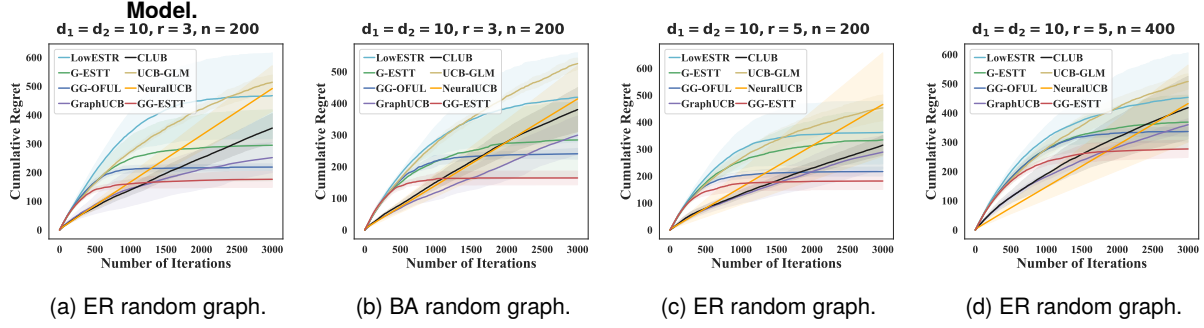
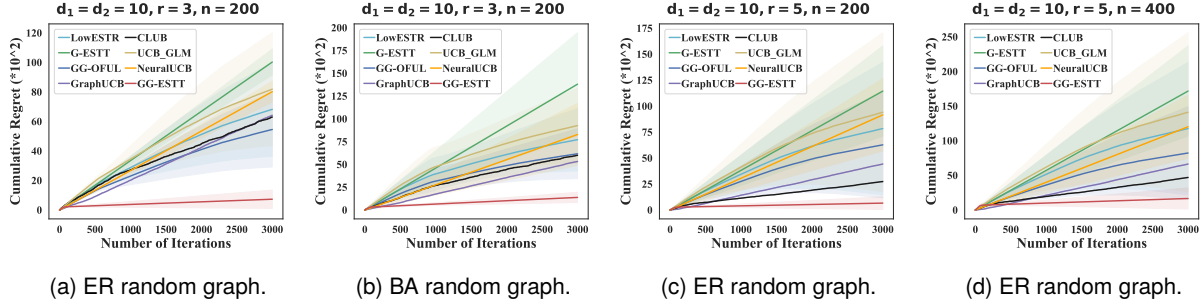
Figure 4 Linear Case: Comparison of Regret in Four Different Settings about r, n , and Random Graph Model.

indicates that larger graph model parameter lead to richer similarity information in the graph, which facilitates more accurate subspace estimation and faster identification of the best arms, thereby improving the overall decision-making performance. This empirical result is consistent with our theoretical analysis, where graph information plays a key role in reducing regret, further validating the effectiveness of the proposed algorithm in leveraging graph information.

5.1.2. Comparison with State-of-the-Art Algorithms In this subsection, we compare the proposed algorithm with several representative and publicly available bandit algorithms, including those that focus on low-rank structure, those that utilize graph information, and classical vector-based algorithms without any additional structural information. The comprehensive list is as follows.

- GG-ESTT (this paper): Algorithm 1.
- LowESTR (Lu et al. 2021): the matrix UCB algorithm based on low-rank subspace exploration.
- G-ESTT (Kang et al. 2022): the generalized linear matrix UCB algorithm based on low-rank subspace exploration.
- GG-OFUL (Algorithm 3 in Appendix F): the vectorized version of the proposed GG-ESTT.
- GraphUCB (Yang et al. 2020): the graph based UCB algorithm via regularization.
- CLUB (Gentile et al. 2014): the graph based UCB algorithm via clustering.
- UCB-GLM (Li et al. 2017): the generalized linear version of the UCB algorithm.
- NeuralUCB (Zhou et al. 2020a): the neural network based UCB algorithm.

In this set of simulations, we consider four different settings that vary in terms of the rank r of the parameter matrix Θ^* , the number of actions n , and the type of random graph model used. These experimental results are shown in Figure 4 (linear case), Figure 5 (binary logistic case) and Figure 6 (poisson case). Clearly, in these four different settings, our proposed GG-ESTT algorithm outperforms other algorithms in terms of cumulative regret. Additionally, we observed that our algorithm achieves faster to obtain sub-linear performance. Compared to the two algorithms in the low-rank matrix setting, these advantages indicate that the first stage obtained a more accurate

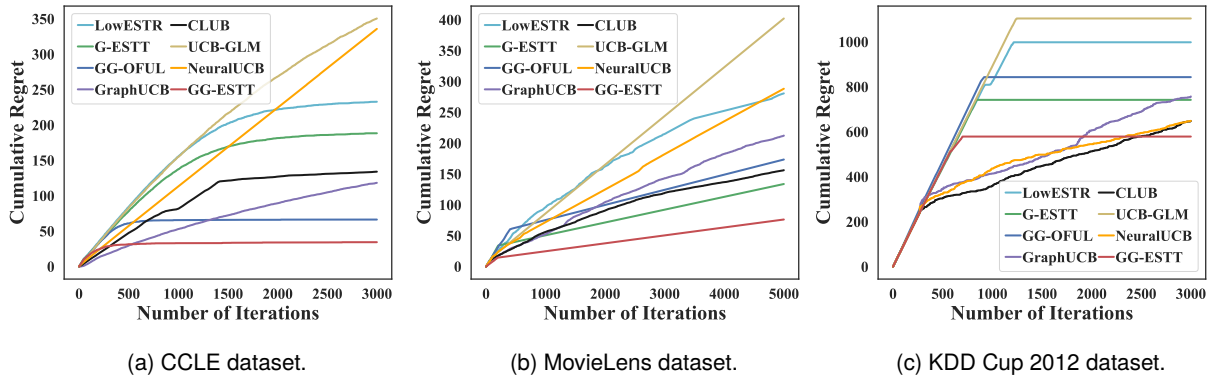
Figure 5 Binary Logistic Case: Comparison of Regret in Four Different Settings about r, n , and Random Graph**Figure 6 Poisson Case: Comparison of Regret in Four Different Settings about r, n , and Random Graph Model.**

estimation of the parameter subspace. This is consistent with our theory, suggesting that GG-ESTT not only leverages the low-rank structure, but also integrates graph information, thus improving the accuracy of estimating the parameter Θ^* and providing better guidance for subsequent decisions. Compared to algorithms in the vector setting, this advantage suggests that data vectorization impairs its inherent low-rank structure, affecting the effectiveness of the estimation and subsequently influencing the action selection process.

5.2. Real-World Data Experiments

To better highlight the outstanding performance of our algorithm, we consider three real-world applications involving cancer treatment (linear case), movie recommendation (binary logistic case), and ad searches (poisson case). To enhance the persuasiveness of our experiments, we use publicly available datasets for each application and apply the following preprocessing steps:

- The Cancer Cell Line Encyclopedia (CCLE) dataset¹: We perform data normalization due to significant differences in data ranges. We consider the (cell line, target) pair as an action, involving 20 cell lines and 17 targets, resulting in 340 actions. The reward is given by the corresponding drug sensitivity measurements.
- The MovieLens dataset²: We address missing values by imputing them with zeros. We treat the (user, movie) pair as an action. To minimize the proportion of missing data, we select the top

Figure 7 Comparison of Regret on Three Real-World Datasets.

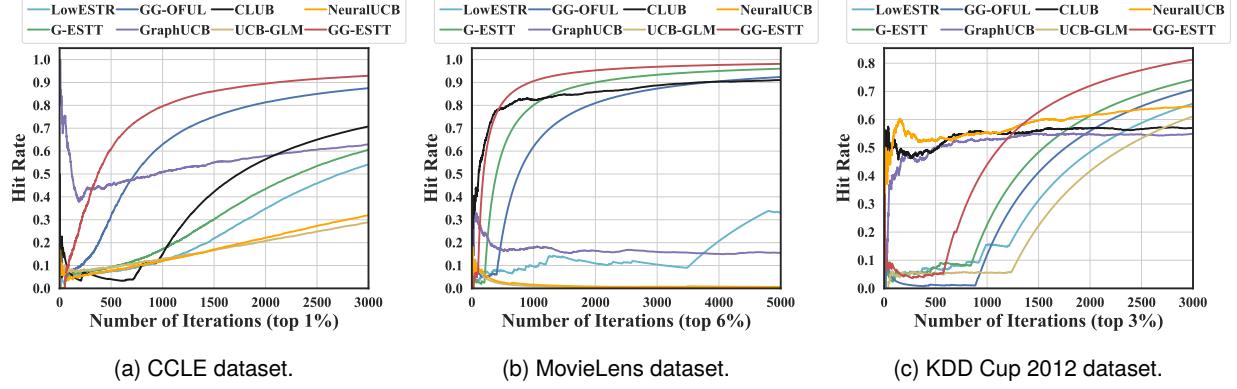
20 active users and movies, forming 400 actions. The reward is set to 1 if the user’s rating for the movie is greater than 3, and 0 otherwise.

- The KDD Cup 2012 dataset³: We address missing values by imputing them with zeros. We treat the (ad, search keywords) pair as an action, involving 20 ads and 13 search keywords, resulting in 260 actions. The reward is the ad’s impression, which refers to the total number of times the ad has been viewed.

We model the rewards as the corresponding matrix R and perform SVD of $R = F_1 \Theta^* F_2^\top$. We then define $\{X_l = F_1[i, :] \odot F_2[j, :] : l = (i - 1)n_2 + j \in \{1, \dots, n\}, i \in \{1, \dots, n_1\}, j \in \{1, \dots, n_2\}\}$ as the action set and Θ^* as the true parameter, where n_1 is the number of item 1, n_2 is the number of item 2, the number of (item 1, item 2) is $n \triangleq n_1 n_2$. In contrast to simulated experiments, for real-world data, we construct the corresponding graph \mathcal{G} using the 5-nearest neighbor method.

The cumulative regret as a standard metric to measure the reward gap between the algorithm’s decisions and the optimal ones. In other words, a smaller cumulative regret indicates that the algorithm is making more accurate decisions. From Figure 7, it is evident that over a certain period, the proposed GG-ESTT algorithm can achieve sublinear regret more rapidly, while also having the smallest cumulative regret. In other words, compared to other algorithms, our approach leverages the inherent structure (graph information and low-rankness) of the dataset more effectively, allowing for a better estimation of the parameter Θ^* , and consequently, delivering superior performance.

In addition, we further illustrate the performance of our algorithm by visualizing the Hit Rate (Yi et al. 2024), which quantifies the frequency of the optimal action selected over time and is defined as $\text{Hit Rate}(t) \triangleq \frac{1}{t} \sum_{i=1}^t \mathbb{I}(h_i \in \mathcal{H})$, where h_i denotes the action selected at time i , and \mathcal{H} represents the set of optimal actions (i.e., the set of actions ranked in the top $x\%$ in terms of rewards). As shown in Figure 8, our algorithm consistently achieves the highest hit rate across all three real-world

Figure 8 Comparison of Hit Rate on Three Real-World Datasets.

datasets. Moreover, the Hit Rate gradually approaches 1 as the number of iterations increases, further demonstrating the effectiveness of our algorithm in selecting optimal actions.

6. Conclusion

This study tackles the practical needs of complex decision-making scenarios where both the low-rank matrix structure and graph information are available. Precisely, we introduce the nuclear norm and a newly designed graph Laplacian regularization to capture these two types of underlying structural information and devise a graph-based action selection strategy based on the UCB principle. By representing the sum of such two regularizers as an equivalent atomic norm, we are able to directly leverage existing analytical frameworks to derive a better cumulative regret bound compared with the popular alternatives. Specifically, the numerator of this bound includes a factor that reflects the richness of the graph information, which decreases as more graph information becomes available, thereby highlighting the significant role of utilizing graph information in decision-making. In future work, we are trying to extend this presented study to dynamic or unknown graph settings, thereby improving its applicability and generalization capabilities.

Notes

¹See <https://depmap.org/portal/download/>.

²See <https://grouplens.org/datasets/movielens/>.

³See <http://www.kddcup2012.org/c/kddcup2012-track2/>.

References

- Abbasi-Yadkori Y, Pál D, Szepesvári C (2011) Improved algorithms for linear stochastic bandits. *Advances in Neural Information Processing Systems* 24:2312–2320.
- Abdallah T, Farzaneh MA, Venkataraman A (2025) Leveraging assortment similarities for data-driven demand prediction. Available at SSRN 5133673 .

- Agrawal P, Tulabandhula T, Avadhanula V (2023) A tractable online learning algorithm for the multinomial logit contextual bandit. *European Journal of Operational Research* 310(2):737–750.
- Aramayo N, Schiappacasse M, Goic M (2023) A multi-armed bandit approach for house ads recommendations. *Marketing Science* 42(2):271–292.
- Bastani H, Bayati M (2020) Online decision making with high-dimensional covariates. *Operations Research* 68(1):276–294.
- Bastani H, Harsha P, Perakis G, Singhvi D (2022) Learning personalized product recommendations with customer disengagement. *Manufacturing & Service Operations Management* 24(4):2010–2028.
- Cai J, Chen R, Wainwright MJ, Zhao L (2023) Doubly high-dimensional contextual bandits: an interpretable model for joint assortment-pricing. *arXiv preprint arXiv:2309.08634* .
- Cesa-Bianchi N, Gentile C, Zappella G (2013) A gang of bandits. *Advances in Neural Information Processing Systems* 26:737–745.
- Chen X, Wang Y, Zhou Y (2020) Dynamic assortment optimization with changing contextual information. *Journal of Machine Learning Research* 21(216):1–44.
- Chu W, Li L, Reyzin L, Schapire R (2011) Contextual bandits with linear payoff functions. *International Conference on Artificial Intelligence and Statistics*, 208–214 (PMLR).
- Gentile C, Li S, Kar P, Karatzoglou A, Zappella G, Etrue E (2017) On context-dependent clustering of bandits. *International Conference on Machine Learning*, 1253–1262 (PMLR).
- Gentile C, Li S, Zappella G (2014) Online clustering of bandits. *International conference on Machine Learning*, 757–765 (PMLR).
- Gong X, Zhang J (2025) Efficient graph bandit learning with side-observations and switching constraints. *Proceedings of the AAAI Conference on Artificial Intelligence*, 16871–16879.
- Gou Y, Yi J, Zhang L (2023) Stochastic graphical bandits with heavy-tailed rewards. *Uncertainty in Artificial Intelligence*, 734–744 (PMLR).
- Han K, He Y, Liu AX, Tang S, Huang H (2020) Differentially private and budget-limited bandit learning over matroids. *INFORMS Journal on Computing* 32(3):790–804.
- Han X, Wang L, Fan W (2023) Cost-effective social media influencer marketing. *INFORMS Journal on Computing* 35(1):138–157.
- Jang K, Jun KS, Yun SY, Kang W (2021) Improved regret bounds of bilinear bandits using action space analysis. *International Conference on Machine Learning*, 4744–4754 (PMLR).
- Jang K, Zhang C, Jun KS (2024) Efficient low-rank matrix estimation, experimental design, and arm-set-dependent low-rank bandits. *arXiv preprint arXiv:2402.11156* .
- Jun KS, Bhargava A, Nowak R, Willett R (2017) Scalable generalized linear bandits: online computation and hashing. *Advances in Neural Information Processing Systems* 30:99–109.

- Jun KS, Willett R, Wright S, Nowak R (2019) Bilinear bandits with low-rank structure. *International Conference on Machine Learning*, 3163–3172 (PMLR).
- Kang Y, Hsieh CJ, Lee TCM (2022) Efficient frameworks for generalized low-rank matrix bandit problems. *Advances in Neural Information Processing Systems* 35:19971–19983.
- Kang Y, Hsieh CJ, Lee TCM (2024) Low-rank matrix bandits with heavy-tailed rewards. *Uncertainty in Artificial Intelligence*, 1863–1889 (PMLR).
- Katariya S, Kveton B, Szepesvari C, Vernade C, Wen Z (2017) Stochastic rank-1 bandits. *International Conference on Artificial Intelligence and Statistics*, 392–401 (PMLR).
- Kocák T, Munos R, Kveton B, Agrawal S, Valko M (2020) Spectral bandits. *The Journal of Machine Learning Research* 21(1):9003–9046.
- Korda N, Szorenyi B, Li S (2016) Distributed clustering of linear bandits in peer to peer networks. *International Conference on Machine Learning*, 1301–1309 (PMLR).
- Kveton B, Szepesvári C, Rao A, Wen Z, Abbasi-Yadkori Y, Muthukrishnan S (2017) Stochastic low-rank bandits. *arXiv preprint arXiv:1712.04644*.
- Lee SJ, Sun WW, Liu Y (2024) Low-rank online dynamic assortment with dual contextual information. *arXiv preprint arXiv:2404.17592*.
- LeJeune D, Dasarathy G, Baraniuk R (2020) Thresholding graph bandits with graph. *International Conference on Artificial Intelligence and Statistics*, 2476–2485 (PMLR).
- Li L, Chu W, Langford J, Schapire RE (2010) A contextual-bandit approach to personalized news article recommendation. *Proceedings of the 19th International Conference on World Wide Web*, 661–670.
- Li L, Lu Y, Zhou D (2017) Provably optimal algorithms for generalized linear contextual bandits. *International Conference on Machine Learning*, 2071–2080 (PMLR).
- Li S, Karatzoglou A, Gentile C (2016) Collaborative filtering bandits. *Proceedings of the 39th International ACM SIGIR conference on Research and Development in Information Retrieval*, 539–548.
- Lu Y, Meisami A, Tewari A (2021) Low-rank generalized linear bandit problems. *International Conference on Artificial Intelligence and Statistics*, 460–468 (PMLR).
- Minsker S (2018) Sub-gaussian estimators of the mean of a random matrix with heavy-tailed entries. *The Annals of Statistics* 46(6A):2871–2903.
- Plan Y, Vershynin R (2016) The generalized lasso with non-linear observations. *IEEE Transactions on Information Theory* 62(3):1528–1537.
- Qi Y, Ban Y, He J (2022) Neural bandit with arm group graph. *Proceedings of the 28th ACM SIGKDD Conference on Knowledge Discovery and Data Mining*, 1379–1389.
- Qi Y, Ban Y, He J (2023) Graph neural bandits. *Proceedings of the 29th ACM SIGKDD Conference on Knowledge Discovery and Data Mining*, 1920–1931.

- Rao N, Yu HF, Ravikumar PK, Dhillon IS (2015) Collaborative filtering with graph information: consistency and scalable methods. *Advances in Neural Information Processing Systems* 28:2107–2115.
- Thaker P, Malu M, Rao N, Dasarathy G (2022) Maximizing and satisficing in multi-armed bandits with graph information. *Advances in Neural Information Processing Systems* 35:2019–2032.
- Trinh C, Kaufmann E, Vernade C, Combes R (2020) Solving bernoulli rank-one bandits with unimodal thompson sampling. *International Conference on Algorithmic Learning Theory*, 862–889 (PMLR).
- Wang Z, Xie J, Liu X, Li S, Lui J (2023) Online clustering of bandits with misspecified user models. *Advances in Neural Information Processing Systems* 36:3785–3818.
- Yang K, Toni L (2018) Graph-based recommendation system. *2018 IEEE Global Conference on Signal and Information Processing (GlobalSIP)*, 798–802 (IEEE).
- Yang K, Toni L, Dong X (2020) Laplacian-regularized graph bandits: algorithms and theoretical analysis. *International Conference on Artificial Intelligence and Statistics*, 3133–3143 (PMLR).
- Yang Z, Balasubramanian K, Liu H (2017) High-dimensional non-gaussian single index models via thresholded score function estimation. *International Conference on Machine Learning*, 3851–3860 (PMLR).
- Yi Q, Yang Y, Tang S, Liu J, Wang Y (2024) Effective generalized low-rank tensor contextual bandits. *IEEE Transactions on Knowledge and Data Engineering* 36(12):8051–8065.
- Zhou D, Li L, Gu Q (2020a) Neural contextual bandits with ucb-based exploration. *International Conference on Machine Learning*, 11492–11502 (PMLR).
- Zhou F, Zhang K, Xie S, Luo X (2020b) Learning to correlate accounts across online social networks: an embedding-based approach. *INFORMS Journal on Computing* 32(3):714–729.
- Zhou T, Wang Y, Yan L, Tan Y (2023) Spoiled for choice? personalized recommendation for healthcare decisions: a multi-armed bandit approach. *Information Systems Research* 34(4):1493–1512.

Supplemental Material for “Generalized Low-Rank Matrix Contextual Bandits with Graph Information”

This supplementary material provides the complete proofs of the theoretical results presented in the main manuscript, including Lemma 1 and Theorems 1–4, along with the corresponding technical lemmas required in the analysis. In addition, due to space limitations in the main text, we also include a detailed description of the vectorized version of the GG-ESTT introduced in Algorithm 3.

Appendix A: Proof of the Lemma 1

The Lemma 1 represents the first key step in this work, providing an equivalent reformulation of the sum of two regularization terms as an atomic norm. To elaborate on this result, we introduce the following Lemma A.1.

LEMMA A.1 (Corollary 1 in Rao et al. (2015)). *Let $L_w = U_w S_w U_w^\top$, $L_h = U_h S_h U_h^\top$ be the full SVD decomposition of L_w, L_h , respectively. Defined $\mathcal{A} \triangleq \{\omega_i h_i^\top : \omega_i = A u_i, h_i = B v_i, \|u_i\| = \|v_i\| = 1, A = U_w S_w^{-1/2}, B = U_h S_h^{-1/2}\}$, then*

$$\|Z\|_{\mathcal{A}} = \inf_{W, H} \frac{1}{2} \left\{ \text{tr}(W^\top L_w W) + \text{tr}(H^\top L_h H) \right\},$$

where $Z = WH^\top$.

Proof of Lemma 1 Perform the full SVD of Θ , denoted as $\Theta = U_\Theta S_\Theta V_\Theta^\top$. Define $W = U_\Theta S_\Theta^{1/2}$ and $H = V_\Theta S_\Theta^{1/2}$, then it follows that $\Theta = WH^\top$. Let $L_h = \lambda I, 2a_\mu \alpha (H^\top \otimes I) \tilde{X}^\top L \tilde{X} (H \otimes I) + \lambda I = I \otimes L_w$, then the sum of the regularization terms in Equation (3) can be rewritten as

$$\begin{aligned} & \lambda \|\Theta\|_* + a_\mu \alpha \text{tr} \left\{ \Theta^\top \tilde{X}^\top L \tilde{X} \Theta \right\} \\ &= \frac{\lambda}{2} \left\{ \|W\|_F^2 + \|H\|_F^2 \right\} + a_\mu \alpha \text{vec}^\top(WH^\top) \tilde{X}^\top L \tilde{X} \text{vec}(WH^\top) \\ &= \frac{\lambda}{2} \left\{ \text{vec}^\top(W) \text{vec}(W) + \text{vec}^\top(H) \text{vec}(H) \right\} + a_\mu \alpha \text{vec}^\top(W) [(H^\top \otimes I) \tilde{X}^\top L \tilde{X} (H \otimes I)] \text{vec}(W) \\ &= \frac{1}{2} \text{vec}^\top(H) (\lambda I) \text{vec}(H) + \text{vec}^\top(W) \left(a_\mu \alpha (H^\top \otimes I) \tilde{X}^\top L \tilde{X} (H \otimes I) + \lambda I \right) \text{vec}(W) \\ &= \frac{1}{2} \text{vec}^\top(H) (I \otimes L_h) \text{vec}(H) + \frac{1}{2} \text{vec}^\top(W) (I \otimes L_w) \text{vec}(W) \\ &= \frac{1}{2} \text{tr} \{ H^\top L_h H \} + \frac{1}{2} \text{tr} \{ W^\top L_w W \}, \end{aligned} \tag{10}$$

where the i -th row of the matrix \tilde{X} corresponds to the vectorization of the i -th action. Then, according to Lemma A.1, we have $\|\Theta\|_{\mathcal{A}} = \inf_{\Theta} \left\{ \lambda \|\Theta\|_* + a_\mu \alpha \text{tr} \left\{ \Theta^\top \tilde{X}^\top L \tilde{X} \Theta \right\} \right\}$. \square

Appendix B: Proof of the Theorem 1

In this section, we will provide a detailed proof of Theorem 1. The basic framework of the proof is as follows.

- Step 1: Drawing on the idea of Rao et al. (2015), we equivalently transform the sum of the two regularizations into an atomic norm, leading to Lemma 1.
- Step 2: Building on the first step, we adopt the proof framework proposed by Kang et al. (2022), handling the regularization term and the loss function separately, which correspond to Lemma B.1 and Lemma B.2, respectively. Finally, we derive the bound for the parameter estimation error.
- Step 3: To demonstrate the improvement of the bound, we need to verify that the additional factor related to graph information in the bound is less than 1, as shown in Lemma B.3.

First, we introduce the relevant lemmas, with their detailed proofs provided in subsection B.1-B.3.

LEMMA B.1. For $\Theta^* = AMB^\top$, where the definitions of A and B can be found in Lemma 1, the low-rank matrix $M \stackrel{SYD}{=} (U, U_\perp) \Sigma^* (V, V_\perp)^\top$, let $\Theta = \hat{\Theta} - \mu^* \Theta^*$,

$$\Lambda_1 = \begin{pmatrix} 0 & 0 \\ 0 & U_\perp^\top A^{-1} \Theta B^{-\top} V_\perp \end{pmatrix}, \quad \Lambda_2 = \begin{pmatrix} U^\top A^{-1} \Theta B^{-\top} V & U^\top A^{-1} \Theta B^{-\top} V_\perp \\ U_\perp^\top A^{-1} \Theta B^{-\top} V & 0 \end{pmatrix}, \quad (11)$$

then

- $\|\mu^* \Theta^*\|_{\mathcal{A}} - \|\hat{\Theta}\|_{\mathcal{A}} \leq \|A(U, U_\perp) \Lambda_2 (V, V_\perp)^\top B^\top\|_{\mathcal{A}} - \|A(U, U_\perp) \Lambda_1 (V, V_\perp)^\top B^\top\|_{\mathcal{A}};$
- $\|\hat{\Theta} - \mu^* \Theta^*\|_{\mathcal{A}} = \|A(U, U_\perp) \Lambda_1 (V, V_\perp)^\top B^\top\|_{\mathcal{A}} + \|A(U, U_\perp) \Lambda_2 (V, V_\perp)^\top B^\top\|_{\mathcal{A}}.$

LEMMA B.2. For the loss function defined as $L_{T_1}(\Theta) \triangleq \langle \Theta, \Theta \rangle - \frac{2}{T_1} \sum_{i=1}^{T_1} \langle \psi_\nu(y_i \cdot S(X_i)), \Theta \rangle$, then use

$$\beta = \frac{4\|A\|\|B\|}{\sqrt{T_1}} \sqrt{2d_1 d_2 \gamma (4\omega^2 + r_{\max}^2) \log\left(\frac{2(d_1 + d_2)}{\delta}\right)}, \quad \nu = \sqrt{\frac{2 \log\left(\frac{2(d_1 + d_2)}{\delta}\right)}{T_1 d_1 d_2 \gamma (4\omega^2 + r_{\max}^2)}},$$

with probability at least $1 - \delta$, we have $\beta \geq 2\|\nabla L(\mu^* \Theta^*)\|_{\mathcal{A}}^*$, where $\|\cdot\|_{\mathcal{A}}^*$ is the dual norm of the weighted atomic norm $\|\cdot\|_{\mathcal{A}}$.

LEMMA B.3. Let $\lambda \leq 1$, $\alpha \leq \frac{1-\lambda}{4a_\mu n(n-1)}$, then $\|A^{-1}\| \leq 1$, $\|B^{-1}\| \leq 1$.

Next, we will complete the proof of Theorem 1 by following the steps summarized above and using the corresponding lemmas.

Proof of Theorem 1 According to the optimal problem and Taylor's expansion, we have

$$\begin{cases} L(\hat{\Theta}) + \beta \|\hat{\Theta}\|_{\mathcal{A}} \leq L(\mu^* \Theta^*) + \beta \|\mu^* \Theta^*\|_{\mathcal{A}}, & \text{optimal problem} \\ L(\hat{\Theta}) = L(\mu^* \Theta^*) + \langle \nabla L(\mu^* \Theta^*), \hat{\Theta} - \mu^* \Theta^* \rangle + 2\|\hat{\Theta} - \mu^* \Theta^*\|_F^2. & \text{Taylor's expansion} \end{cases}$$

Then, by swapping the order, we obtain

$$\|\hat{\Theta} - \mu^* \Theta^*\|_F^2 \leq -\frac{1}{2} \langle \nabla L(\mu^* \Theta^*), \hat{\Theta} - \mu^* \Theta^* \rangle + \frac{\beta}{2} [\|\mu^* \Theta^*\|_{\mathcal{A}} - \|\hat{\Theta}\|_{\mathcal{A}}]. \quad (12)$$

Next, by Cauchy-Schwarz inequality, (12) can be further expressed as

$$\|\hat{\Theta} - \mu^* \Theta^*\|_F^2 \leq \frac{1}{2} \|\nabla L(\mu^* \Theta^*)\|_{\mathcal{A}}^* \|\hat{\Theta} - \mu^* \Theta^*\|_{\mathcal{A}} + \frac{\beta}{2} [\|\mu^* \Theta^*\|_{\mathcal{A}} - \|\hat{\Theta}\|_{\mathcal{A}}]. \quad (13)$$

Due to Lemma B.1, we can get

$$\begin{aligned} \|\hat{\Theta} - \mu^* \Theta^*\|_F^2 &\leq \frac{1}{2} [\|\nabla L(\mu^* \Theta^*)\|_{\mathcal{A}}^* + \beta] \|A(U, U_\perp) \Lambda_2 (V, V_\perp)^\top B^\top\|_{\mathcal{A}} \\ &\quad + \frac{1}{2} [\|\nabla L(\mu^* \Theta^*)\|_{\mathcal{A}}^* - \beta] \|A(U, U_\perp) \Lambda_1 (V, V_\perp)^\top B^\top\|_{\mathcal{A}}. \end{aligned} \quad (13)$$

Due to Lemma B.2, we can get

$$\begin{aligned} \|\hat{\Theta} - \mu^* \Theta^*\|_F^2 &\leq \frac{3}{4} \beta \|A(U, U_\perp) \Lambda_2 (V, V_\perp)^\top B^\top\|_{\mathcal{A}} - \frac{1}{4} \beta \|A(U, U_\perp) \Lambda_1 (V, V_\perp)^\top B^\top\|_{\mathcal{A}} \\ &\leq \frac{3}{4} \beta \|A(U, U_\perp) \Lambda_2 (V, V_\perp)^\top B^\top\|_{\mathcal{A}} \\ &\leq \frac{3}{4} \beta \|\Lambda_2\|_* \leq \frac{3}{4} \beta \sqrt{2r} \|\Lambda_2\|_F \leq \frac{3}{4} \beta \sqrt{2r} \|\Lambda\|_F \\ &\leq \frac{3}{4} \beta \sqrt{2r} \|A^{-1}(\hat{\Theta} - \mu^* \Theta^*) B^{-\top}\|_F \\ &\leq \frac{3}{4} \beta \sqrt{2r} \|A^{-1}\| \|\hat{\Theta} - \mu^* \Theta^*\|_F \|B^{-\top}\| \\ &\leq \frac{3}{4} \beta \sqrt{2r} \|\hat{\Theta} - \mu^* \Theta^*\|_F, \end{aligned} \quad (14)$$

that is $\|\hat{\Theta} - \mu^* \Theta^*\|_F \leq \frac{3}{4} \beta \sqrt{2r} = \frac{6\sqrt{\gamma(4\omega^2 + r_{\max}^2)} \|A\| \|B\| \sqrt{d_1 d_2 r \log\left(\frac{2(d_1 + d_2)}{\delta}\right)}}{\sqrt{T_1}}$. Due to Lemma B.3, we have $\|A\| \leq \|A^{-1}\| \leq 1$ and $\|B\| \leq \|B^{-1}\| \leq 1$. Then letting $\zeta \triangleq \|A\| \|B\|$, we can obtain $\zeta \in (0, 1]$. \square

B.1. Proof of the Lemma B.1

Proof of Theorem B.1 According to Definition 3, we can deduce that $\Theta^* = \sum_i c_i A u_i v_i^\top B^\top \triangleq A M B^\top$, simultaneously satisfying $\text{rank}(M) = \text{rank}(\Theta^*) = r$. Therefore, we can conclude that $\Theta^* \in \mathcal{M} = \{A M B^\top : \text{rank}(M) = r, A = U_w S_w^{\frac{1}{2}}, B = U_h S_h^{\frac{1}{2}}\}$. Let $M = U \Sigma V^\top$ be the truncated SVD, where $U \in \mathbb{R}^{d_1 \times r}$, $V \in \mathbb{R}^{d_2 \times r}$. Then

$$\Theta^* = A (U, U_\perp) \begin{pmatrix} \Sigma & 0 \\ 0 & 0 \end{pmatrix} (V, V_\perp)^\top B^\top = A (U, U_\perp) \Sigma^* (V, V_\perp)^\top B^\top, \quad (15)$$

where $U_\perp \in \mathbb{R}^{d_1 \times (d_1 - r)}$, $\Sigma^* \in \mathbb{R}^{d_1 \times d_2}$ and $V_\perp \in \mathbb{R}^{d_2 \times (d_2 - r)}$. Furthermore, we define $\Lambda = (U, U_\perp)^\top A^{-1} \Theta B^{-\top} (V, V_\perp) = \Lambda_1 + \Lambda_2$, where let $\Theta = \widehat{\Theta} - \mu^* \Theta^*$,

$$\Lambda_1 = \begin{pmatrix} 0 & 0 \\ 0 & U_\perp^\top A^{-1} \Theta B^{-\top} V_\perp \end{pmatrix}, \quad \Lambda_2 = \begin{pmatrix} U^\top A^{-1} \Theta B^{-\top} V & U^\top A^{-1} \Theta B^{-\top} V_\perp \\ U_\perp^\top A^{-1} \Theta B^{-\top} V & 0 \end{pmatrix}, \quad (16)$$

i.e. $\Theta = A (U, U_\perp) \Lambda (V, V_\perp)^\top B^\top$. Please note that we can express $\|Z\|_{\mathcal{A}}$ of Lemma A.1 as follows:

$$\begin{aligned} \|Z\|_{\mathcal{A}} &= \inf_{W, H} \frac{1}{2} \{ \text{tr}(W^\top L_w W) + \text{tr}(H^\top L_h H) \} = \inf_{W, H} \frac{1}{2} \{ \|A^{-1} W\|_F^2 + \|B^{-1} H\|_F^2 \} \\ &= \inf_{W, H} \{ \|A^{-1} W (B^{-1} H)^\top\|_* \} = \|A^{-1} Z B^{-\top}\|_*. \end{aligned} \quad (17)$$

On the one hand, for $\|\mu^* \Theta^*\|_{\mathcal{A}} - \|\widehat{\Theta}\|_{\mathcal{A}}$, it holds that

$$\begin{aligned} \|\widehat{\Theta}\|_{\mathcal{A}} &= \|\mu^* \Theta^* + \Theta\|_{\mathcal{A}} = \|A^{-1} (\mu^* \Theta^* + \Theta) B^{-\top}\|_* = \|\mu^* \Sigma^* + \Lambda\|_* \\ &= \|\mu^* \Sigma^* + \Lambda_1 + \Lambda_2\|_* \geq \|\mu^* \Sigma^* + \Lambda_1\|_* - \|\Lambda_2\|_* = \|\mu^* \Sigma^*\|_* + \|\Lambda_1\|_* - \|\Lambda_2\|_* \\ &= \|A^{-1} (A (U, U_\perp) \mu^* \Sigma^* (V, V_\perp)^\top B^\top) B^{-\top}\|_* + \|A^{-1} (A (U, U_\perp) \Lambda_1 (V, V_\perp)^\top B^\top) B^{-\top}\|_* \\ &\quad - \|A^{-1} (A (U, U_\perp) \Lambda_2 (V, V_\perp)^\top B^\top) B^{-\top}\|_* \\ &= \|A (U, U_\perp) \mu^* \Sigma^* (V, V_\perp)^\top B^\top\|_{\mathcal{A}} + \|A (U, U_\perp) \Lambda_1 (V, V_\perp)^\top B^\top\|_{\mathcal{A}} - \|A (U, U_\perp) \Lambda_2 (V, V_\perp)^\top B^\top\|_{\mathcal{A}} \\ &= \|\mu^* \Theta^*\|_{\mathcal{A}} + \|A (U, U_\perp) \Lambda_1 (V, V_\perp)^\top B^\top\|_{\mathcal{A}} - \|A (U, U_\perp) \Lambda_2 (V, V_\perp)^\top B^\top\|_{\mathcal{A}}, \end{aligned} \quad (18)$$

which implies that $\|\mu^* \Theta^*\|_{\mathcal{A}} - \|\widehat{\Theta}\|_{\mathcal{A}} \leq \|A (U, U_\perp) \Lambda_2 (V, V_\perp)^\top B^\top\|_{\mathcal{A}} - \|A (U, U_\perp) \Lambda_1 (V, V_\perp)^\top B^\top\|_{\mathcal{A}}$.

On the other hand, for $\|\widehat{\Theta} - \mu^* \Theta^*\|_{\mathcal{A}}$, we can obtain

$$\begin{aligned} \|\widehat{\Theta} - \mu^* \Theta^*\|_{\mathcal{A}} &= \|\Theta\|_{\mathcal{A}} = \|A (U, U_\perp) \Lambda (V, V_\perp)^\top B^\top\|_{\mathcal{A}} = \|A^{-1} (A (U, U_\perp) \Lambda (V, V_\perp)^\top B^\top) B^{-\top}\|_* \\ &= \|\Lambda_1 + \Lambda_2\|_* = \|\Lambda_1\|_* + \|\Lambda_2\|_* = \|A^{-1} (A (U, U_\perp) \Lambda_1 (V, V_\perp)^\top B^\top) B^{-\top}\|_* \\ &\quad + \|A^{-1} (A (U, U_\perp) \Lambda_2 (V, V_\perp)^\top B^\top) B^{-\top}\|_* \\ &= \|A (U, U_\perp) \Lambda_1 (V, V_\perp)^\top B^\top\|_{\mathcal{A}} + \|A (U, U_\perp) \Lambda_2 (V, V_\perp)^\top B^\top\|_{\mathcal{A}}. \end{aligned} \quad (19)$$

□

B.2. Proof of the Lemma B.2

This subsection aims to prove the relationship between the norm of the gradient of the loss function (specifically, the dual norm of the regularization norm) and the adjusted parameter, as stated in the Lemma B.2. Before formally presenting the proof of the Lemma B.2, it is necessary to clarify the form of the dual norm of the atomic norm, as stated in Lemma B.4.

LEMMA B.4 (Rao et al. (2015)). *The dual norm of the weighted atomic norm in Definition 3 is $\|Z\|_{\mathcal{A}}^* = \|A^\top Z B\|$.*

In addition, despite the difference in the regularization norm between this paper and Kang et al. (2022), the corresponding loss function is the same. Therefore, in the proof, we shall utilize a conclusion from that paper, which we present as follows.

LEMMA B.5 (Lemma B.4 in Kang et al. (2022)). $L : \mathbb{R}^{d_1 \times d_2} \rightarrow \mathbb{R}$ is the loss function defined as $L_{T_1}(\Theta) \triangleq \langle \Theta, \Theta \rangle - \frac{2}{T_1} \sum_{i=1}^{T_1} \langle \psi_{\nu}(y_i \cdot S(X_i)), \Theta \rangle$. Then by setting

$$t = \sqrt{2d_1 d_2 \gamma (4\omega^2 + r_{\max}^2) \log \left(\frac{2(d_1 + d_2)}{\delta} \right)}, \quad \nu = \frac{t}{(4\omega^2 + r_{\max}^2) \gamma d_1 d_2 \sqrt{T_1}} = \sqrt{\frac{2 \log \left(\frac{2(d_1 + d_2)}{\delta} \right)}{T_1 d_1 d_2 \gamma (4\omega^2 + r_{\max}^2)}},$$

we have with probability at least $1 - \delta$, it holds that $P \left(\|\nabla L(\mu^* \Theta^*)\| \geq \frac{2t}{\sqrt{T_1}} \right) \leq \delta$, where $\mu^* = \mathbb{E}[\mu'(\langle X, \Theta^* \rangle)]$.

Proof of Lemma B.2

$$\begin{aligned} P \left(\|\nabla L(\mu^* \Theta^*)\|_{\mathcal{A}}^* \geq \frac{\beta}{2} \right) &= P \left(\|A^\top \nabla L(\mu^* \Theta^*) B\| \geq \frac{\beta}{2} \right) \\ &\leq P \left(\|A\| \|\nabla L(\mu^* \Theta^*)\| \|B\| \geq \frac{\beta}{2} \right) = P \left(\|\nabla L(\mu^* \Theta^*)\| \geq \frac{\beta}{2 \|A\| \|B\|} \right). \end{aligned} \quad (20)$$

Then according to Lemma B.5, let $\beta = \frac{4\|A\|\|B\|}{\sqrt{T_1}} \sqrt{2d_1 d_2 \gamma (4\omega^2 + r_{\max}^2) \log \left(\frac{2(d_1 + d_2)}{\delta} \right)}$, we have completed the proof of Lemma B.2. \square

B.3. Proof the Lemma B.3

The proof process of the Lemma B.3 will involve some fundamental facts about the singular values. To this end, we describe it as follows:

- For any matrix A, B , $\sigma_i(A^\top B) \leq \sigma_i(A) \sigma_1(B)$, where $\sigma_i(\cdot)$ is the i -th largest singular value.
- For any matrix $A \in \mathbb{R}^{n \times n}$, $B \in \mathbb{R}^{p \times p}$, let $\lambda_1, \lambda_2, \dots, \lambda_n$ be the singular values of A , $\mu_1, \mu_2, \dots, \mu_p$ be the singular values of B . Then the singular values of $A \otimes B$ are $\lambda_i \mu_j$, $i = 1, 2, \dots, n$, $j = 1, 2, \dots, p$.
- For any Laplacian matrix L , $\sigma_{\min}(L) = 0$.
- For the graph Laplacian $L = D - W$, $\sigma_{\max}(L) \leq 2d_{\max} \leq 2(n - 1)$, where $d_{\max} = \max_i \sum_j W_{ij}$ is the maximum node degree, n is the number of nodes.

Proof of Lemma B.3 According to the definition of B in Lemma 1, we have $\|B^{-1}\| = \|(U_h S_h^{-\frac{1}{2}})^{-1}\| = \|S_h^{\frac{1}{2}}\| = \sigma_{\max} \left(S_h^{\frac{1}{2}} \right) = \sigma_{\max}^{\frac{1}{2}}(S_h) = \sigma_{\max}^{\frac{1}{2}}(L_h) = \sigma_{\max}^{\frac{1}{2}}(\lambda I) = \lambda^{\frac{1}{2}}$. Let $\lambda \leq 1$, then $\|B^{-1}\| \leq 1$. Similarly, we can obtain $\|A^{-1}\| =$

$\|(U_w S_w^{-\frac{1}{2}})^{-1}\| = \|S_w^{\frac{1}{2}} U_w\| = \|S_w^{\frac{1}{2}}\| = \sigma_{\max}\left(S_w^{\frac{1}{2}}\right) = \sigma_{\max}^{\frac{1}{2}}(S_w) = \sigma_{\max}^{\frac{1}{2}}(L_w)$. Next, we further bound $\sigma_{\max}(L_w)$ by

$$\begin{aligned}
\sigma_{\max}(L_w) &= \sigma_{\max}(I \otimes L_w) = \sigma_{\max}\left(2a_\mu \alpha (H^\top \otimes I) \tilde{X}^\top L \tilde{X} (H \otimes I) + \lambda I\right) \\
&= 2a_\mu \alpha \sigma_{\max}\left((H^\top \otimes I) \tilde{X}^\top L \tilde{X} (H \otimes I)\right) + \lambda \\
&\leq 2a_\mu \alpha \sigma_{\max}(H^\top \otimes I) \sigma_{\max}\left(\tilde{X}^\top L \tilde{X} (H \otimes I)\right) + \lambda \\
&\leq 2a_\mu \alpha \sigma_{\max}(H^\top \otimes I) \sigma_{\max}\left(\tilde{X}^\top L \tilde{X}\right) \sigma_{\max}(H \otimes I) + \lambda \\
&\leq 2a_\mu \alpha \sigma_{\max}(H^\top \otimes I) \sigma_{\max}\left(\tilde{X}^\top\right) \sigma_{\max}(L) \sigma_{\max}(\tilde{X}) \sigma_{\max}(H \otimes I) + \lambda \\
&= 2a_\mu \alpha \sigma_{\max}^2(H) \sigma_{\max}^2(\tilde{X}) \sigma_{\max}(L) + \lambda \\
&= 2a_\mu \alpha \sigma_{\max}^2\left(V_\Theta S_\Theta^{\frac{1}{2}}\right) \sigma_{\max}^2(\tilde{X}) \sigma_{\max}(L) + \lambda \\
&= 2a_\mu \alpha \sigma_{\max}^2(\Theta) \sigma_{\max}^2(\tilde{X}) \sigma_{\max}(L) + \lambda \\
&\leq 2a_\mu \alpha \|\Theta\|_F \sigma_{\max}^2(\tilde{X}) \sigma_{\max}(L) + \lambda \\
&\leq 2a_\mu \alpha \sigma_{\max}^2(\tilde{X}) \sigma_{\max}(L) + \lambda,
\end{aligned} \tag{21}$$

where the condition for the last inequality to hold is the assumption $\|\Theta\|_F \leq 1$ made without loss of generality. Then, letting

$$\alpha \leq \frac{1 - \lambda}{2a_\mu \sigma_{\max}^2(\tilde{X}) \sigma_{\max}(L)}, \tag{22}$$

we have $\|A^{-1}\| = \sigma_{\max}^{\frac{1}{2}}(L_w) \leq 1$. For practical purposes, using the bounds $\sigma_{\max}^2(\tilde{X}) \leq \|\tilde{X}\|_F^2 \leq n$, $\sigma_{\max}(L) \leq 2(n-1)$, we further relax the condition to $\alpha \leq \frac{1-\lambda}{4a_\mu n(n-1)}$, to avoid the explicit computation of singular values.

□

Appendix C: Proof of the Theorem 2

Theorem 2 delineates the confidence interval of expected reward. In its proof, we primarily rely on the Fundamental Theorem of Calculus and inequalities involving weighted norm, thereby breaking it down into two components involving noise and true parameter. The proofs of these two components are associated with the following two lemmas, respectively.

LEMMA C.1 (Lemma C.3 in Kang et al. (2022)). *Let $\{F_t\}_{t=0}^\infty$ be a filtration and $\{\eta_t\}_{t=1}^\infty$ be a real-valued stochastic process such that η_t is F_t -measurable and η_t is conditionally ω -sub-Gaussian for some $\omega \geq 0$ i.e.*

$$\forall \lambda \in \mathbb{R}, \mathbb{E}\left[e^{\lambda \eta_t} \mid F_{t-1}\right] \leq \exp\left(\frac{\lambda^2 \omega^2}{2}\right).$$

Let $\{\mathbf{x}_t\}_{t=1}^\infty$ be an \mathbb{R}^d -valued stochastic process such that \mathbf{x}_t is F_{t-1} -measurable. Assume that V is a $d \times d$ positive definite matrix and independent with sample random variables after time m . For any $t \geq 2$, define

$$\bar{V}_t = V + \sum_{s=1}^t \mathbf{x}_s \mathbf{x}_s^\top \quad \mathbf{s}_t = \sum_{s=1}^t \eta_s \mathbf{x}_s.$$

Then, for any $\delta > 0$, with probability at least $1 - \delta$, for all $t \geq m + 1$,

$$\|\mathbf{s}_t\|_{\bar{V}_t^{-1}}^2 \leq \omega^2 \log\left(\frac{|\bar{V}_t|}{|V| \delta^2}\right).$$

LEMMA C.2 (Lemma 16 in Kocák et al. (2020)). For any symmetric, positive semi-definite matrix X , and any vectors \mathbf{u} and \mathbf{y} , $\mathbf{y}^\top (X + \mathbf{u}\mathbf{u}^\top)^{-1} \mathbf{y} \leq \mathbf{y}^\top X^{-1} \mathbf{y}$.

Proof of Theorem 2 First, we appropriately scale $\left| \mu(\mathbf{x}^\top \boldsymbol{\theta}^*) - \mu(\mathbf{x}^\top \hat{\boldsymbol{\theta}}_t) \right|$. According to the Fundamental Theorem of Calculus, we have $\left| \mu(\mathbf{x}^\top \boldsymbol{\theta}^*) - \mu(\mathbf{x}^\top \hat{\boldsymbol{\theta}}_t) \right| \leq k_\mu \left| \mathbf{x}^\top (\boldsymbol{\theta}^* - \hat{\boldsymbol{\theta}}_t) \right|$, i.e. $\mu(\cdot)$ is k_μ -Lipshitz continuous. Applying this theorem again, let $G_t = \int_0^1 g'_t \left(s\boldsymbol{\theta}^* + (1-s)\hat{\boldsymbol{\theta}}_t \right) ds$, where $g_t(\boldsymbol{\theta}) = \sum_{i=1}^{T_1} \mu(\mathbf{x}_{h,i}^\top \boldsymbol{\theta}) \mathbf{x}_{h,i} + \sum_{i=1}^{t-1} \mu(\mathbf{x}_i^\top \boldsymbol{\theta}) \mathbf{x}_i + \Lambda \boldsymbol{\theta} + a_\mu \alpha \tilde{X}^\top L \tilde{X} \boldsymbol{\theta}$, we obtain $\left| \mathbf{x}^\top (\boldsymbol{\theta}^* - \hat{\boldsymbol{\theta}}_t) \right| = \left| \mathbf{x}^\top G_t^{-1} (g_t(\boldsymbol{\theta}^*) - g_t(\hat{\boldsymbol{\theta}}_t)) \right|$. Due to the Cauchy-Schwarz inequality, we can obtain

$$\left| \mathbf{x}^\top G_t^{-1} (g_t(\boldsymbol{\theta}^*) - g_t(\hat{\boldsymbol{\theta}}_t)) \right| \leq \|\mathbf{x}\|_{G_t^{-1}} \|G_t^{-1} (g_t(\boldsymbol{\theta}^*) - g_t(\hat{\boldsymbol{\theta}}_t))\|_{G_t} = \|\mathbf{x}\|_{G_t^{-1}} \|g_t(\boldsymbol{\theta}^*) - g_t(\hat{\boldsymbol{\theta}}_t)\|_{G_t^{-1}}. \quad (23)$$

Combining the above inequalities, we obtain $\left| \mu(\mathbf{x}^\top \boldsymbol{\theta}^*) - \mu(\mathbf{x}^\top \hat{\boldsymbol{\theta}}_t) \right| \leq k_\mu \|\mathbf{x}\|_{G_t^{-1}} \|g_t(\boldsymbol{\theta}^*) - g_t(\hat{\boldsymbol{\theta}}_t)\|_{G_t^{-1}}$.

According to $g'_t(\boldsymbol{\theta}) = \sum_{i=1}^{T_1} \mu'(\mathbf{x}_{h,i}^\top \boldsymbol{\theta}) \mathbf{x}_{h,i} \mathbf{x}_{h,i}^\top + \sum_{k=1}^{t-1} \mu'(\mathbf{x}_k^\top \boldsymbol{\theta}) \mathbf{x}_k \mathbf{x}_k^\top + \Lambda + a_\mu \alpha \tilde{X}^\top L \tilde{X} \geq c_\mu V_t(c_\mu)$, then we have $G_t \geq c_\mu V_t(c_\mu)$, that is $G_t^{-1} \leq \frac{V_t^{-1}(c_\mu)}{c_\mu}$. In addition, based on the definition of $g_t(\cdot)$, we have $g_t(\boldsymbol{\theta}^*) - g_t(\hat{\boldsymbol{\theta}}_t) = -\sum_{k=1}^{T_1} \epsilon_{h,k} \mathbf{x}_{h,k} - \sum_{k=1}^{t-1} \epsilon_k \mathbf{x}_k - \Lambda \boldsymbol{\theta}^* - a_\mu \alpha \tilde{X}^\top L \tilde{X} \boldsymbol{\theta}^*$. Based on the above processing, we have

$$\begin{aligned} \left| \mu(\mathbf{x}^\top \boldsymbol{\theta}^*) - \mu(\mathbf{x}^\top \hat{\boldsymbol{\theta}}_t) \right| &\leq k_\mu \|\mathbf{x}\|_{G_t^{-1}} \|g_t(\boldsymbol{\theta}^*) - g_t(\hat{\boldsymbol{\theta}}_t)\|_{G_t^{-1}} \\ &\leq \frac{k_\mu}{c_\mu} \|\mathbf{x}\|_{V_t^{-1}(c_\mu)} \left[\left\| \sum_{k=1}^{T_1} \epsilon_{h,k} \mathbf{x}_{h,k} + \sum_{k=1}^{t-1} \epsilon_k \mathbf{x}_k \right\|_{V_t^{-1}(c_\mu)} + \left\| \Lambda \boldsymbol{\theta}^* + a_\mu \alpha \tilde{X}^\top L \tilde{X} \boldsymbol{\theta}^* \right\|_{V_t^{-1}(c_\mu)} \right]. \end{aligned} \quad (24)$$

Next, we will separately handle the two terms inside the brackets in the above inequality. Specifically for the term $\left\| \sum_{k=1}^{T_1} \epsilon_{h,k} \mathbf{x}_{h,k} + \sum_{k=1}^{t-1} \epsilon_k \mathbf{x}_k \right\|_{V_t^{-1}(c_\mu)}$, directly applying Lemma C.1 yields

$$\left\| \sum_{k=1}^{T_1} \epsilon_{h,k} \mathbf{x}_{h,k} + \sum_{k=1}^{t-1} \epsilon_k \mathbf{x}_k \right\|_{V_t^{-1}(c_\mu)} \leq \omega \sqrt{\log \left(\frac{|V_t(c_\mu)|}{|V(c_\mu)| \delta^2} \right)}. \quad (25)$$

For the term $\left\| (\Lambda + a_\mu \alpha \tilde{X}^\top L \tilde{X}) \boldsymbol{\theta}^* \right\|_{V_t^{-1}(c_\mu)}$, we have

$$\begin{aligned} \left\| (\Lambda + a_\mu \alpha \tilde{X}^\top L \tilde{X}) \boldsymbol{\theta}^* \right\|_{V_t^{-1}(c_\mu)} &= \sqrt{\boldsymbol{\theta}^{*\top} (\Lambda + a_\mu \alpha \tilde{X}^\top L \tilde{X}) V_t^{-1}(c_\mu) (\Lambda + a_\mu \alpha \tilde{X}^\top L \tilde{X}) \boldsymbol{\theta}^*} \\ &\leq \sqrt{c_\mu \boldsymbol{\theta}^{*\top} (\Lambda + a_\mu \alpha \tilde{X}^\top L \tilde{X}) \boldsymbol{\theta}^*} = \sqrt{c_\mu (\boldsymbol{\theta}^{*\top} \Lambda \boldsymbol{\theta}^* + \boldsymbol{\theta}^{*\top} a_\mu \alpha \tilde{X}^\top L \tilde{X} \boldsymbol{\theta}^*)} \\ &= \sqrt{c_\mu \left(\lambda_2 \sum_{i=1}^k \boldsymbol{\theta}_i^{*2} + \lambda_\perp \sum_{i=k+1}^{d_1 d_2} \boldsymbol{\theta}_i^{*2} + \boldsymbol{\theta}^{*\top} a_\mu \alpha \tilde{X}^\top L \tilde{X} \boldsymbol{\theta}^* \right)} \\ &\leq \sqrt{c_\mu (\lambda_2 + \lambda_\perp \tau^2 + a_\mu \alpha \sigma_{\max}(\tilde{X}^\top L \tilde{X}))} \leq \sqrt{c_\mu} \left[\sqrt{\lambda_2} + \sqrt{\lambda_\perp} \tau + \sqrt{a_\mu \alpha \sigma_{\max}(\tilde{X}^\top L \tilde{X})} \right] \\ &\leq \sqrt{c_\mu} \left(\sqrt{\lambda_2} + \sqrt{\lambda_\perp} \tau + \sqrt{\frac{a_\mu (1-\lambda) \sigma_{\max}(\tilde{X}^\top L \tilde{X})}{2 a_\mu \sigma_{\max}^2(\tilde{X}) \sigma_{\max}(L)}} \right) \\ &\leq \sqrt{c_\mu} (\sqrt{\lambda_2} + \sqrt{\lambda_\perp} \tau + 1), \end{aligned} \quad (26)$$

where the first inequality holds is based on Lemma C.2, the fourth inequality is based on (22).

Finally, substituting (25) and (26) into (24) yields the conclusion of the Theorem 2. \square

Appendix D: Proof of the Theorem 3

Theorem 3 provides the regret bound for the arm selection strategy, and its proof consists of two main steps. First, based on the confidence bound established in Theorem 2 and using Lemmas D.1 and D.2, we derive a regret that includes the term $\log \left(\frac{|V_T(c_\mu)|}{|V(c_\mu)|} \right)$. Second, when further bounding this term, we observe that the matrix $V(c_\mu)$ is no longer diagonal due to the incorporation of graph information, making Lemma 2 in Jun et al. (2019) inapplicable. To address this, we extend the result to the general case of positive definite matrix (as shown in Lemma D.3), and by carefully choosing the parameter λ_\perp , we complete the derivation of the final regret bound.

LEMMA D.1 (Lemma 3 in Jun et al. (2017)).

$$\min\{a, x\} \leq \max\{2, a\} \log(1+x), \forall a, x > 0.$$

LEMMA D.2 (Lemma 11 in Abbasi-Yadkori et al. (2011)). Let $\{\mathbf{x}_t\}_{t=1}^\infty$ be a sequence in \mathbb{R}^d , V is the $d \times d$ positive definite matrix and define $V_t = V + \sum_{s=1}^t \mathbf{x}_s \mathbf{x}_s^\top$. Then, we have that

$$\sum_{t=1}^T \log(1 + \|\mathbf{x}_t\|_{V_t^{-1}}^2) = \log \frac{|V_T|}{|V|}.$$

LEMMA D.3 (The Bound about Matrix Determinant). For any t , let $V_t \triangleq \sum_{s=1}^{t-1} \mathbf{x}_s \mathbf{x}_s^\top + V$, where V is a positive definite matrix. Then,

$$\log \frac{|V_t|}{|V|} \leq \max_{t_i: \sum_{i=1}^{d_1 d_2} t_i = t-1} \sum_{i=1}^{d_1 d_2} \log \left(1 + \frac{t_i}{\sigma_i(V)} \right).$$

Proof of Theorem 3 According to the Cauchy-Schwarz inequality and the relationship among norms, let $e_T = \omega \sqrt{\log \frac{|V_T(c_\mu)|}{|V(c_\mu)| \delta^2} + \sqrt{c_\mu} (\sqrt{\lambda_2} + \sqrt{\lambda_\perp} \tau + 1)}$, we can obtain

$$r_t \triangleq \mu(\langle \mathbf{x}^*, \boldsymbol{\theta}^* \rangle) - \mu(\langle \mathbf{x}_t, \boldsymbol{\theta}^* \rangle) \leq \min \left\{ 2k_\mu, 2\frac{k_\mu}{c_\mu} e_t \|\mathbf{x}_t\|_{V_t^{-1}(c_\mu)} \right\} \leq 2\frac{k_\mu}{c_\mu} e_T \min \left\{ \frac{c_\mu}{e_T}, \|\mathbf{x}_t\|_{V_t^{-1}(c_\mu)} \right\}.$$

By applying the Cauchy-Schwarz inequality again, we can obtain

$$\sum_{t=1}^T r_t \leq \sqrt{T \sum_{t=1}^T r_t^2} \leq 2\frac{k_\mu}{c_\mu} e_T \sqrt{T \sum_{t=1}^T \min \left\{ \frac{c_\mu^2}{e_T^2}, \|\mathbf{x}_t\|_{V_t^{-1}(c_\mu)}^2 \right\}}. \quad (27)$$

Based on Lemma D.1, we can obtain

$$\sum_{t=1}^T r_t \leq 2\frac{k_\mu}{c_\mu} e_T \sqrt{T \max \left\{ 2, \frac{c_\mu^2}{e_T^2} \right\} \sum_{t=1}^T \log \left(1 + \|\mathbf{x}_t\|_{V_t^{-1}(c_\mu)}^2 \right)}. \quad (28)$$

Furthermore, due to Lemma D.2, we have

$$\begin{aligned} \sum_{t=1}^T r_t &\leq 2\frac{k_\mu}{c_\mu} e_T \sqrt{T \max \left\{ 2, \frac{c_\mu^2}{e_T^2} \right\} \log \frac{|V_T(c_\mu)|}{|V(c_\mu) + \sum_{i=1}^{T_1} \mathbf{x}_{h,i} \mathbf{x}_{h,i}^\top|}} \\ &\leq 2\frac{k_\mu}{c_\mu} e_T \sqrt{T \max \left\{ 2, \frac{c_\mu^2}{e_T^2} \right\} \log \frac{|V_T(c_\mu)|}{|V(c_\mu)|}}. \end{aligned} \quad (29)$$

Next, we perform the e_T^2 as

$$\begin{aligned} e_T^2 &= \left(\omega \sqrt{\log \frac{|V_T(c_\mu)|}{|V(c_\mu)|\delta^2}} + \sqrt{c_\mu} (\sqrt{\lambda_2} + \sqrt{\lambda_\perp} \tau + 1) \right)^2 \\ &\geq c_\mu (\sqrt{\lambda_2} + \sqrt{\lambda_\perp} \tau + 1)^2 \geq c_\mu (\lambda_2 + 1). \end{aligned} \quad (30)$$

That is to say, $\frac{c_\mu^2}{e_T^2} \leq \frac{c_\mu}{\lambda_2 + 1} \leq \frac{c_\mu}{\lambda_2}$. By substituting (30) into (29) yields

$$R_T \triangleq \sum_{t=1}^T r_t = O \left(e_T \sqrt{T \log \frac{|V_T(c_\mu)|}{|V(c_\mu)|}} \right). \quad (31)$$

According to the Lemma D.3, we have $\log \frac{|V_T(c_\mu)|}{|V(c_\mu)|} \leq \max_{t_i: \sum_{i=1}^{d_1 d_2} t_i = T-1} \sum_{i=1}^{d_1 d_2} \log \left(1 + \frac{t_i}{\sigma_i(V(c_\mu))} \right)$. Considering that $\sigma_i(V(c_\mu)) = \sigma_i \left(\frac{\Lambda + a_\mu \alpha \tilde{X}^\top L \tilde{X}}{c_\mu} \right) \geq \frac{1}{c_\mu} (\sigma_i(\Lambda) + \sigma_{\min}(a_\mu \alpha \tilde{X}^\top L \tilde{X})) \geq \frac{1}{c_\mu} \sigma_i(\Lambda)$, we can obtain

$$\begin{aligned} \log \frac{|V_T(c_\mu)|}{|V(c_\mu)|} &\leq \max_{i=1}^{d_1 d_2} \sum_{i=1}^{d_1 d_2} \log \left(1 + \frac{c_\mu t_i}{\sigma_i(\Lambda)} \right) \leq \max_{i=1}^k \sum_{i=1}^k \log \left(1 + \frac{c_\mu t_i}{\lambda_2} \right) + \max_{i=k+1}^{d_1 d_2} \sum_{i=k+1}^{d_1 d_2} \log \left(1 + \frac{c_\mu t_i}{\lambda_\perp} \right) \\ &\leq k \log \left(1 + \frac{c_\mu T}{\lambda_2} \right) + \sum_{i=k+1}^{d_1 d_2} \frac{c_\mu t_i}{\lambda_\perp} \leq k \log \left(1 + \frac{c_\mu T}{\lambda_2} \right) + \frac{c_\mu T}{\lambda_\perp}. \end{aligned} \quad (32)$$

If $\lambda_\perp = \frac{c_\mu T}{k \log(1 + c_\mu T / \lambda_2)}$, then $\log \frac{|V_T(c_\mu)|}{|V(c_\mu)|} \leq 2k \log \left(1 + \frac{c_\mu T}{\lambda_2} \right)$. Substituting it into (31), the regret bound is $\tilde{O}(\omega k \sqrt{T} + \tau T)$.

□

D.1. Proof of the Lemma D.3

Lemma D.3 deals with the bound on the determinant ratio of matrices. Due to the incorporation of graph information, the original diagonal matrix in the ratio transforms into a positive definite matrix, rendering the Lemma 2 in Jun et al. (2019) no longer applicable. Therefore, we extend this approach to Lemma D.5, which is primarily based on the fact elucidated in Lemma D.4.

LEMMA D.4 (Lemma 21 in Kocák et al. (2020)). *For any real positive-definite matrix A with only simple eigenvalue multiplicities and any vector \mathbf{x} such that $\|\mathbf{x}\| \leq 1$, we have that the determinant $|A + \mathbf{x}\mathbf{x}^\top|$ is maximized by a vector \mathbf{x} which is aligned with an eigenvector of A .*

LEMMA D.5 (The generalization of Lemma 22 in Kocák et al. (2020)). *Let V be any real positive-definite matrix. For any vectors $\{\mathbf{x}_s\}_{1 \leq s < t}$ such that $\|\mathbf{x}_s\| \leq 1$ for all $1 \leq s < t$, we have that the determinant $|V_t|$ of $V_t \triangleq V + \sum_{s=1}^{t-1} \mathbf{x}_s \mathbf{x}_s^\top$ is maximized when all \mathbf{x}_s are aligned with an eigenvector of V .*

Proof of Lemma D.5 Let $V_t = V_{-t} + \mathbf{x}_t \mathbf{x}_t^\top$, that is $V_{-t} = V + \sum_{s=1}^{t-1} \mathbf{x}_s \mathbf{x}_s^\top$. Next, we will discuss two cases regarding the maximum value of $|V_t|$.

Case 1: all eigenvalues have a multiplicity of 1.

In this scenario, Lemma D.4 can be directly applied, which states that $|V_t|$ achieves its maximum value (maximizing only with respect to \mathbf{x}_t) when an eigenvector of V_{-t} align with \mathbf{x}_t . Therefore, when $|V_t|$ attains its maximum value over all $\{\mathbf{x}_s\}_{s=1}^{t-1}$, each of these \mathbf{x}_s aligns with a corresponding eigenvector of V_{-s} . Due to $V_t \mathbf{x}_i = V_{-t} \mathbf{x}_i + \mathbf{x}_i \mathbf{x}_i^\top \mathbf{x}_i = \sigma_{\min}(V_{-t}) \mathbf{x}_i + \mathbf{x}_i$, these points of maximum values also align with the eigenvectors of V_t . Similarly, according to $V = V_t - \sum_{s=1}^{t-1} \mathbf{x}_s \mathbf{x}_s^\top$, we conclude that all \mathbf{x}_s are aligned with the eigenvectors of V .

Case 2: there exist eigenvalues with multiplicity greater than 1.

In this case, in order to apply Lemma D.4, we introduce a random perturbation with an amplitude not exceeding c . Subsequently, applying Lemma D.4 to the perturbed matrix, we obtain that the determinant $|V_t^c|$ of $V_t^c \triangleq V^c + \sum_{s=1}^{t-1} \mathbf{x}_s^c \mathbf{x}_s^{c\top}$ is maximized when all \mathbf{x}_s^c are aligned with an eigenvector of V^c . Furthermore, due to $\lim_{c \rightarrow 0} |V_t^c| = |V_t|$ and $\lim_{c \rightarrow 0} \mathbf{x}_s^c = \mathbf{x}_s$, therefore when all \mathbf{x}_s are aligned with eigenvectors of V , we can obtain the maximum values of $|V_t|$. \square

Proof of Lemma D.3 We aim to bound the determinant ratio $\frac{|V_t|}{|V|}$ under the conditions $\{\|\mathbf{x}_s\| \leq 1, s = 1, 2, \dots, t-1\}$. To achieve this objective, we first apply Lemma D.5 to obtain an upper bound on $|V_t|$. Let $V = UDU^\top$ be the full SVD, \mathbf{e}_i is the basis vector of the identity matrix, then

$$\begin{aligned} |V_t| &\leq \max_{\substack{\mathbf{x}_1, \dots, \mathbf{x}_{t-1}; \\ \mathbf{x}_s \in \{U\mathbf{e}_1, \dots, U\mathbf{e}_{d_1 d_2}\}}} \left| V + \sum_{s=1}^{t-1} \mathbf{x}_s \mathbf{x}_s^\top \right| = \max_{\substack{\mathbf{x}_1, \dots, \mathbf{x}_{t-1}; \\ \mathbf{x}_s \in \{U\mathbf{e}_1, \dots, U\mathbf{e}_{d_1 d_2}\}}} \left| UDU^\top + \sum_{s=1}^{t-1} U\mathbf{e}_s U\mathbf{e}_s^\top \right| \\ &= \max_{\substack{\sum_{i=1}^{d_1 d_2} t_i = t-1; \\ t_1, \dots, t_{d_1 d_2} \text{ positive integers}}} |\text{diag}(\sigma_i(V) + t_i)| \leq \max_{\substack{\sum_{i=1}^{d_1 d_2} t_i = t-1; \\ t_1, \dots, t_{d_1 d_2} \text{ positive reals}}} \prod_{i=1}^{d_1 d_2} (\sigma_i(V) + t_i). \end{aligned} \quad (33)$$

Furthermore, considering $|V| = |UDU^\top| = \prod_{i=1}^{d_1 d_2} \sigma_i(V)$, we have completed the proof. \square

Appendix E: Proof of the Theorem 4

Proof of Theorem 4 We adjust the scale of the instantaneous regret in the t -th round according to the different stages of the algorithm. In the first stage, i.e., $t \in \{1, 2, \dots, T_1\}$, according to the Fundamental Theorem of Calculus and bounded norm assumption, we have $|\mu(\langle X^*, \Theta^* \rangle) - \mu(\langle X_t, \Theta^* \rangle)| \leq k_\mu |\langle X^* - X_t, \Theta^* \rangle| \leq k_\mu \|X^* - X_t\|_F \|\Theta^*\|_F \leq 2k_\mu$. In the second stage, we can derive the corresponding regret bound based on Theorem 3. We can further obtain the overall regret as follows:

$$\begin{aligned} R_T &= \sum_{t=1}^T \mu(\langle X^*, \Theta^* \rangle) - \mu(\langle X_t, \Theta^* \rangle) \\ &= \sum_{t=1}^{T_1} [\mu(\langle X^*, \Theta^* \rangle) - \mu(\langle X_t, \Theta^* \rangle)] + \sum_{t=1}^{T-T_1} [\mu(\langle X^*, \Theta^* \rangle) - \mu(\langle X_t, \Theta^* \rangle)] \\ &\leq 2k_\mu T_1 + \tilde{O}(\omega k \sqrt{T} + \tau T) \\ &= \tilde{O}\left(\frac{\zeta \sqrt{d_1 d_2 \gamma r T}}{c_r}\right). \end{aligned} \quad (34)$$

\square

Appendix F: GG-OFUL Algorithm

In order to better elucidate the effectiveness of the algorithm proposed in this paper, we vectorize the matrix and deduce the corresponding UCB algorithm via graph Laplacian regularization term defined in Equation (2), naming it GG-OFUL. This algorithm can also be regarded as a vectorized version of the algorithm 1 presented in main text. In this case, this algorithm that corresponds to the estimator $\hat{\theta}_t$ can be obtained by

$$\hat{\theta}_t = \arg \min_{\theta \in \mathbb{R}^{d_1 d_2}} \sum_{i=1}^{T_1} [b(\langle \mathbf{x}_{h,i}, \theta \rangle) - y_{h,i} \langle \mathbf{x}_{h,i}, \theta \rangle] + \sum_{i=1}^{t-1} [b(\langle \mathbf{x}_i, \theta \rangle) - y_i \langle \mathbf{x}_i, \theta \rangle] + \frac{1}{2} \|\theta\|^2 + \frac{\alpha}{2} \theta^\top \tilde{X}^\top L \tilde{X} \theta, \quad (35)$$

where $\mathbf{x}_i \in \mathcal{X}_{\text{vec}} \triangleq \{\text{vec}(X_i) : X_i \in \mathcal{X}\}$. The i -th row of the matrix \tilde{X} corresponds to the i -th action, i.e., \mathbf{x}_i .

Therefore, in the second stage, the main difference from GG-ESTT is that the identity matrix I is replaced with a diagonal matrix Λ . As a result, the algorithm for GG-OFUL is as follows:

Algorithm 3 GG-OFUL**Input:** $\mathcal{X}_{\text{vec}}, T_1, T, L, \alpha, \delta$.

- 1: Let $\bar{V}(c_\mu) = \frac{I + a_\mu \alpha \tilde{X}^\top L \tilde{X}}{c_\mu}$; $\bar{V}_1(c_\mu) = \bar{V}(c_\mu) + \sum_{i=1}^{T_1} \mathbf{x}_{h,i} \mathbf{x}_{h,i}^\top$, where the data $\{\mathbf{x}_{h,i}\}_{i=1}^{T_1}$ collected in the first stage.
- 2: **for** $t = 1$ to T_1 **do**
- 3: Choose action $\mathbf{x}_t \in \mathcal{X}_{\text{vec}}$ according to distribution \mathbb{D} , and receive reward y_t .
- 4: **end for**
- 5: **for** $t = 1$ to $T_2 = T - T_1$ **do**
- 6: Compute $\hat{\theta}_t$ according to Equation (35).
- 7: Choose action $\mathbf{x}_t = \operatorname{argmax}_{\mathbf{x} \in \mathcal{X}_{\text{vec}}} \left\{ \mu \left(\langle \hat{\theta}_t, \mathbf{x} \rangle \right) + \frac{k_\mu}{c_\mu} e_t \|\mathbf{x}\|_{\bar{V}_t^{-1}(c_\mu)} \right\}$ and receive reward y_t ,
 where $e_t = \omega \sqrt{\log \frac{|\bar{V}_t(c_\mu)|}{|\bar{V}(c_\mu)|\delta^2}} + \sqrt{c_\mu} \left(1 + \sqrt{\alpha \sigma_{\max}(\tilde{X}^\top L \tilde{X})} \right)$. The i -th row of the matrix \tilde{X} corresponds to the i -th action, i.e., \mathbf{x}_i .
- 8: Update $\bar{V}_{t+1}(c_\mu) = \bar{V}_t(c_\mu) + \mathbf{x}_t \mathbf{x}_t^\top$.
- 9: **end for**